

SAGEEP 2019

March 2019, Portland, Oregon, USA

Frank Frischknecht Leadership Award keynote address

Recent advances in the geoelectrical method and new challenges

by

M.H. Loke

Geotomo Software Sdn Bhd

Penang, Malaysia.

email : drmhloke@gmail.com

Recent advances in the geoelectrical method and new challenges

Part 1 :- Recent advances

Progress of electrical methods 1910s to 2010s, from 1-D to 4-D.

Part 2 :- New challenges

- (a) Optimized arrays
- (b) Special time-lapse constraints
- (c) Vector surveys
- (d) Structured and unstructured grids
- (e) Affordable tech for emerging countries

Questions

Progress over the last 100 years

From 1-D to 4-D

A centennial snapshot

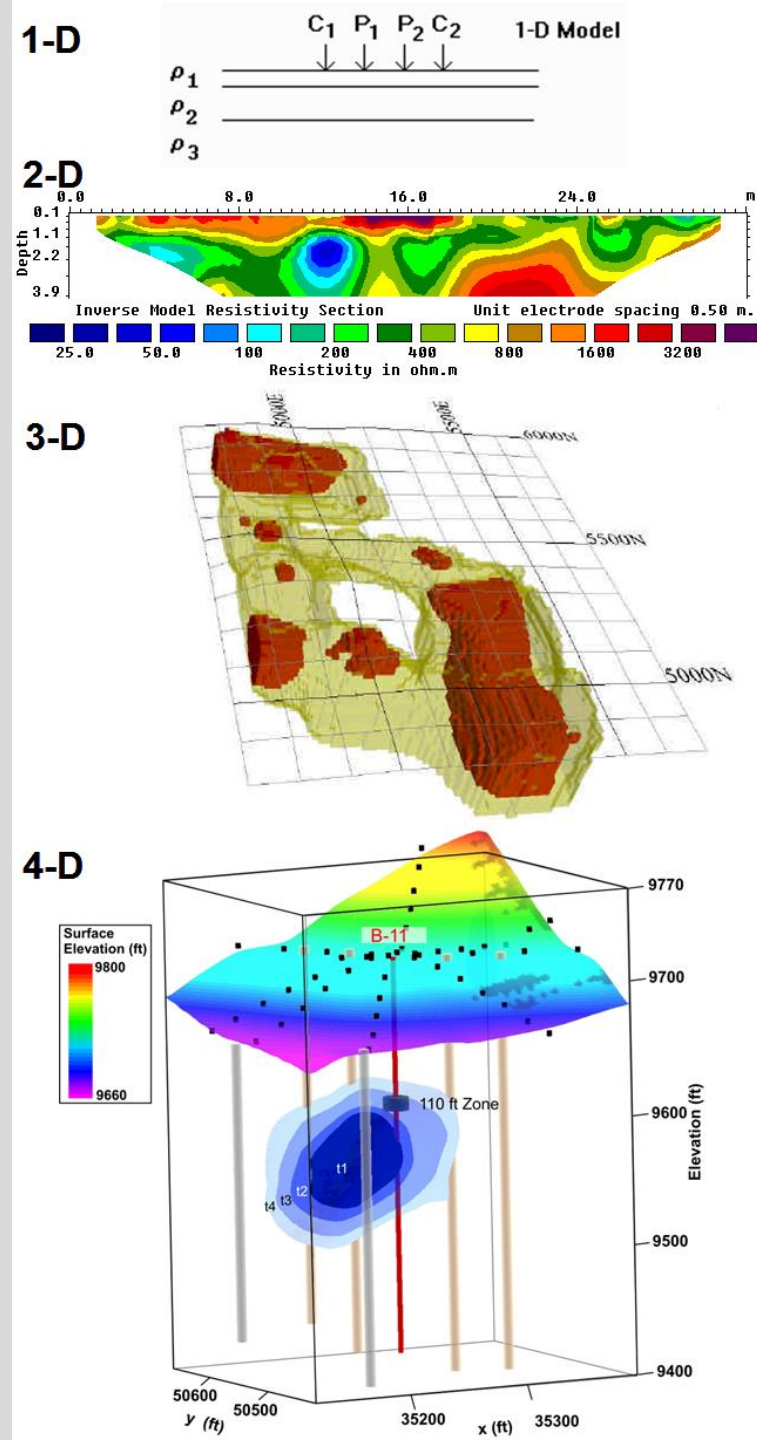
1910s to 1980s : 1-D. Sounding and profiling surveys using resistivity meters with 4 electrodes. Simple models with flat layers.

1990s : 2-D. Major change with multi-electrode systems and fast automatic inversion software for PCs. Birth of a new industry.

2000s : 3-D. Multi-channel meters. Dense areal data coverage. Complex structures.

2010s : 4-D. Environmental monitoring (landslides, aquifers, landfills, dams). Remote systems with wireless control.

Geoelectrics - popular method with low entry barrier. Largest no. papers NSG.



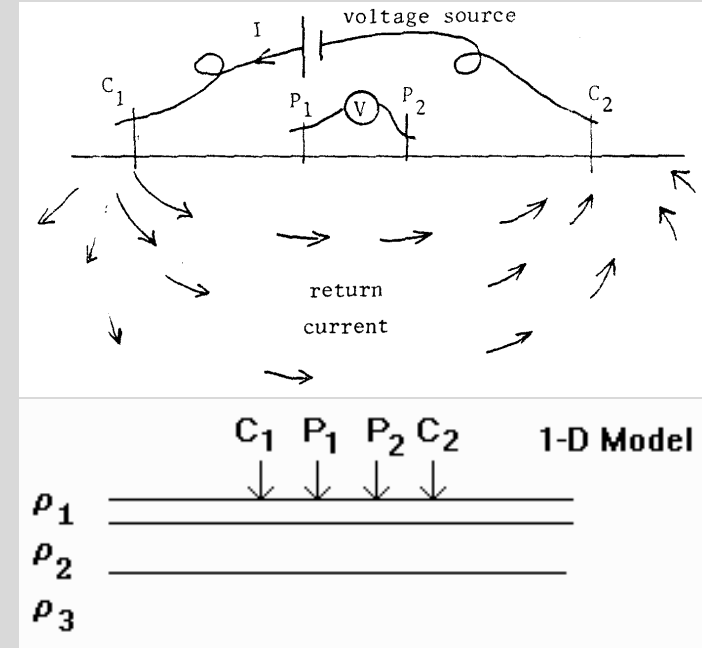
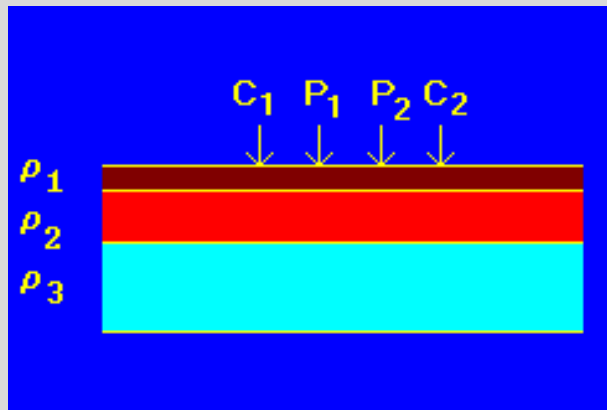
1910s to 1980s : Simple beginnings

1-D sounding surveys with measurements using different spacings between electrodes about the same central point.

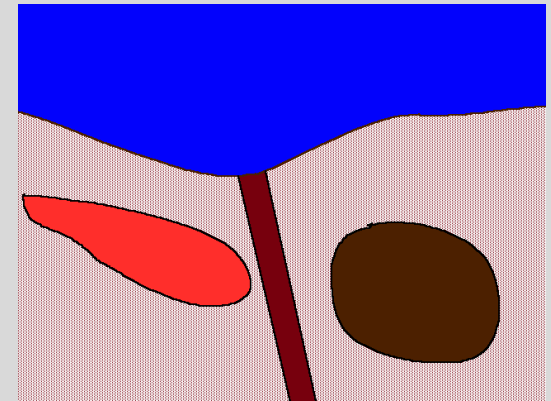
Use a simplified mathematical model that with horizontal layers. Major advance in 1960s with the linear filter method. 1-D inversion with programmable calculators and PCs (1980s).

Traditional resistivity sounding surveys give a 1-D picture of the subsurface, which is too simple in many cases. Problem of model inadequacy.

Sounding 1-D Picture

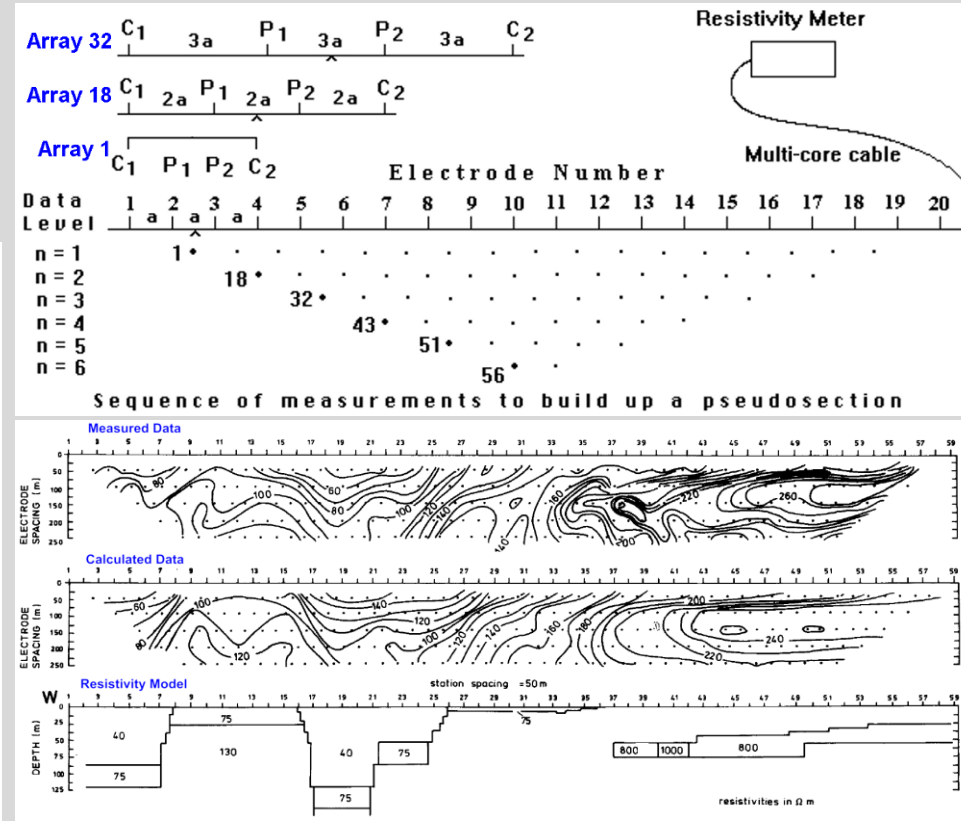
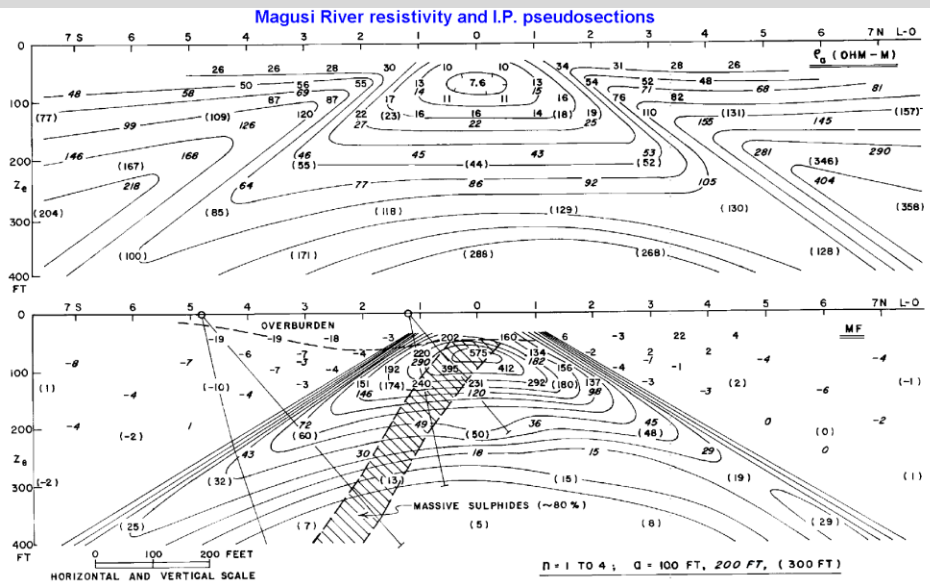


Real Situation



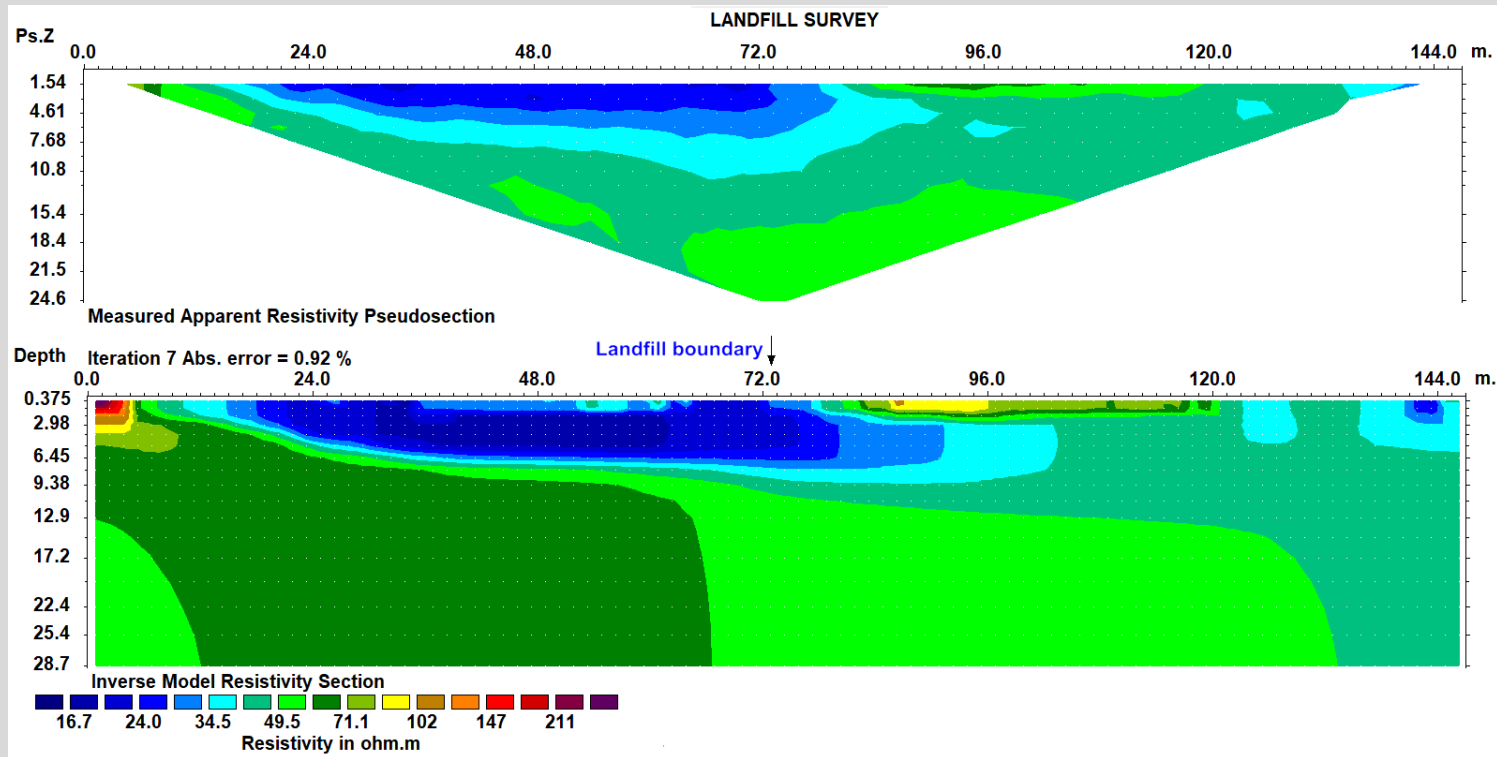
1980 to early 1990s : Through a glass darkly

Since the 1960s, attempts were made to overcome the limitations of 1-D surveys using 2-D measurements, mainly in the mining industry. In the early 1980s microprocessor controlled multi-electrode systems were developed that made 2-D surveys more practical. However, interpretation of the data was rather crude, using the pseudosection contours shapes, or a slow manual refinement of a 2-D forward model taking days.



Mid-1990s : The dawn of a new age

A turning point was in the mid-1990s with a number of commercial and robust multi-electrode systems, and automatic 2-D inversion software that converts the pseudosection data into a model in minutes using inexpensive PCs. This enabled more complex geology to be mapped rapidly and accurately. Lesson – both robust (and inexpensive) hardware and software are needed for a method to be widely used! Data set below was first presented in SAGEEP 1994.



The world is smooth

The smooth-constrained least-squares optimization method is widely used. One version :-

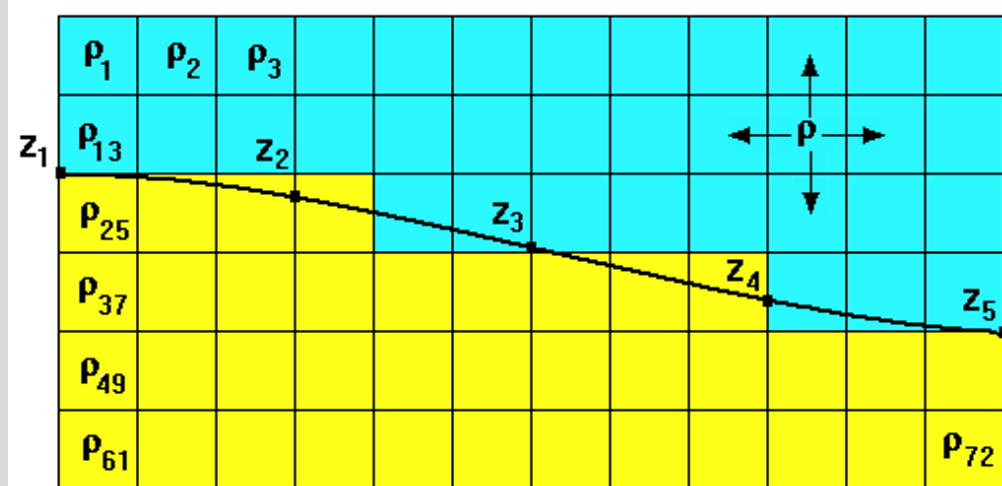
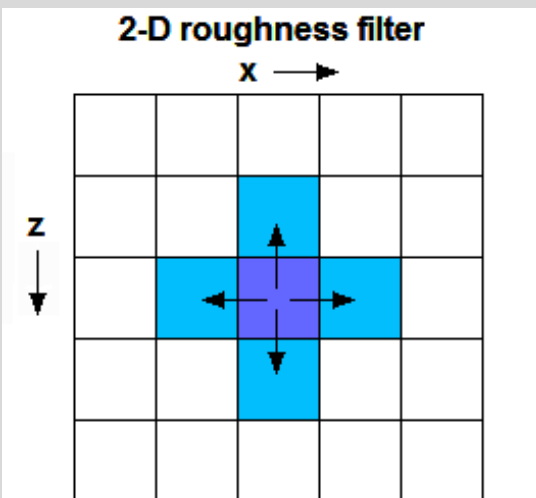
$$[J_i^T R_d J_i + \lambda_i (W^T R_m W + \delta I)] \Delta r_i = J_i^T R_d g_i - \lambda_i [W^T R_m W + \delta I] (r_{i-1} - r_m)$$

r =model value, g =data misfit, J =Jacobian matrix, λ =damping factor

W =roughness filter, r_m = reference model, Δr = change in model

δ =reference model damping factor, R_d, R_m = data weighting, L-norm

Other variations :- Imposing a sharp boundary by breaking coupling across boundary, variable boundary etc.



Hardware : From the four corners of the Earth

There are many commercial multi-electrode systems, with prices from US\$12,000 to \$100,000, cables with 24 to 128 nodes, single and multi channel, with and without I.P. Some systems (Pasi) have both seismic and resistivity functions. Companies :- Abem, Iris Instruments, GF Instruments, Pasi Geophysics, Allied Associates, Siber, ZZ, Geomative, Langeo, Lippmann, Geolog, Scintrex, AGI, OYO, Geometrics

Abem (Sweden)



ZZ (Australia)



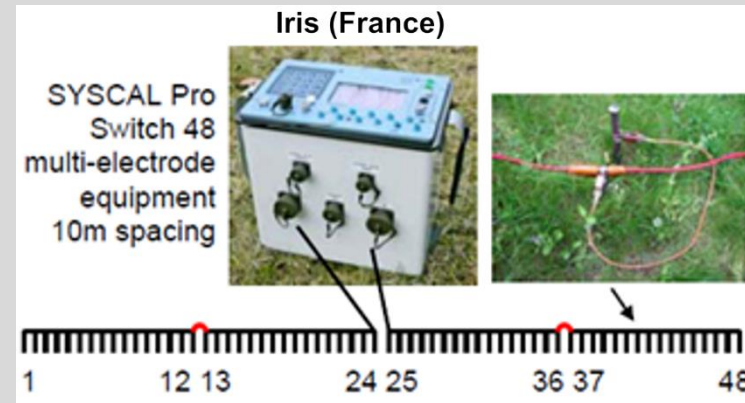
Geomative (China)



Siber (Russia)



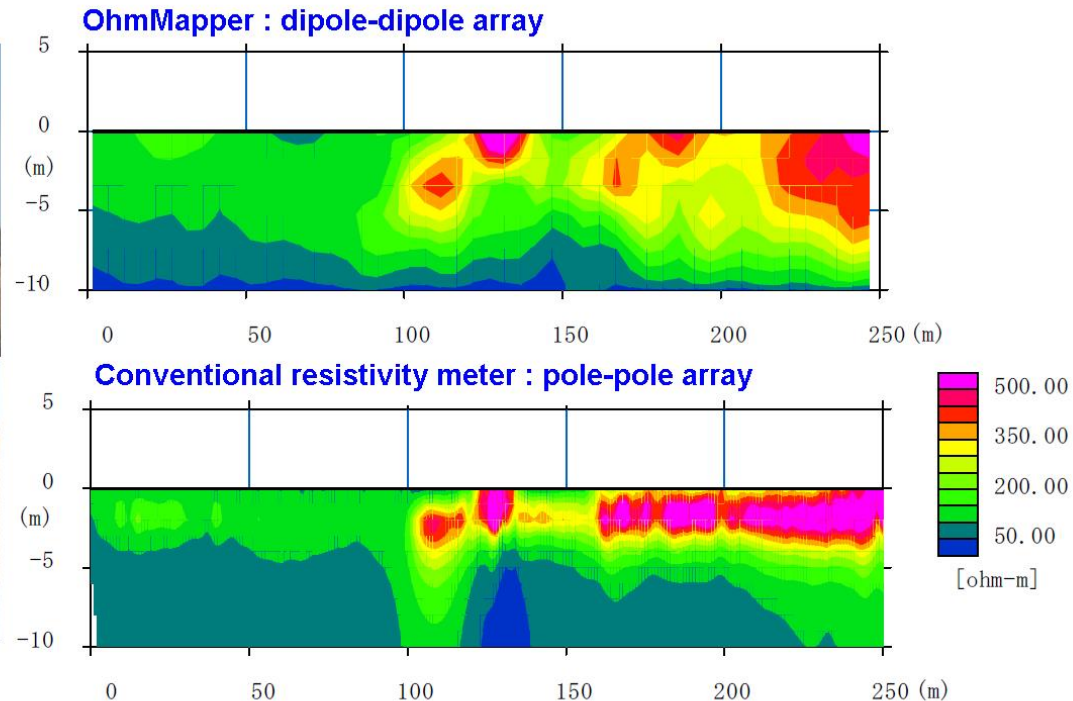
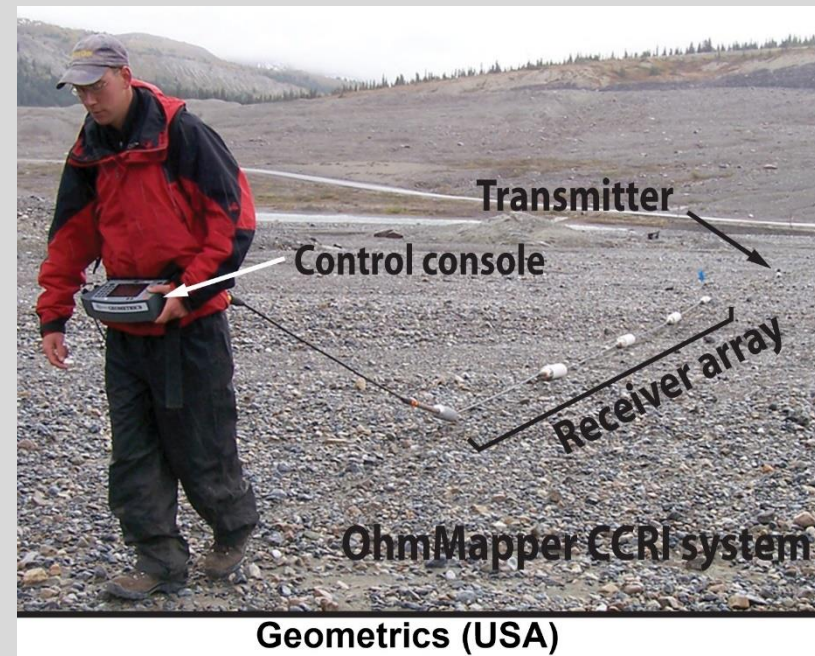
Langeo (China)



Iris (France)

Hardware : It moves

The Geometrics OhmMapper uses a capacitively coupled system that does not require direct ground contact, such as on roads or concrete floors. This system can cover a large area in a short time, but has a more limited depth penetration (3-15m).



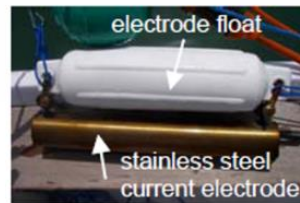
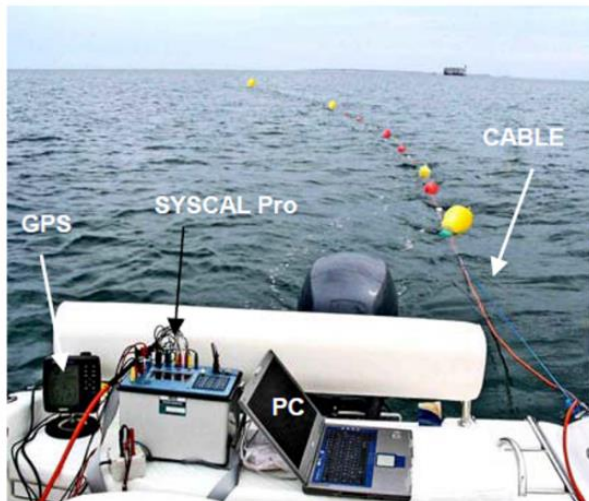
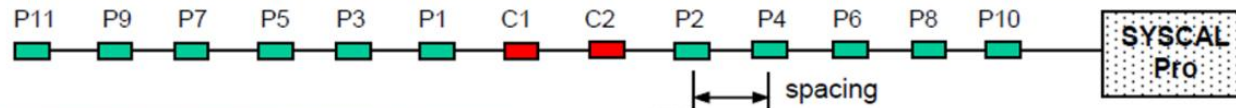
Survey lines on levee (Kokai river, Japan)

Oyo Corporation (Japan) and Geometrics, Inc (USA)

Hardware : Under the sea

Another mobile system is used in aquatic surveys where a streamer is pulled behind a boat. Figure below shows a system with floating electrodes where the line sways to and fro due to water currents. In such cases a 2-D modeling approach is not sufficiently accurate, and a 3-D approach is required. A significant source of 'noise' in aquatic surveys is errors in the electrode positions as they are estimated from a GPS unit on the boat.

SYSCAL Pro for river and sea survey



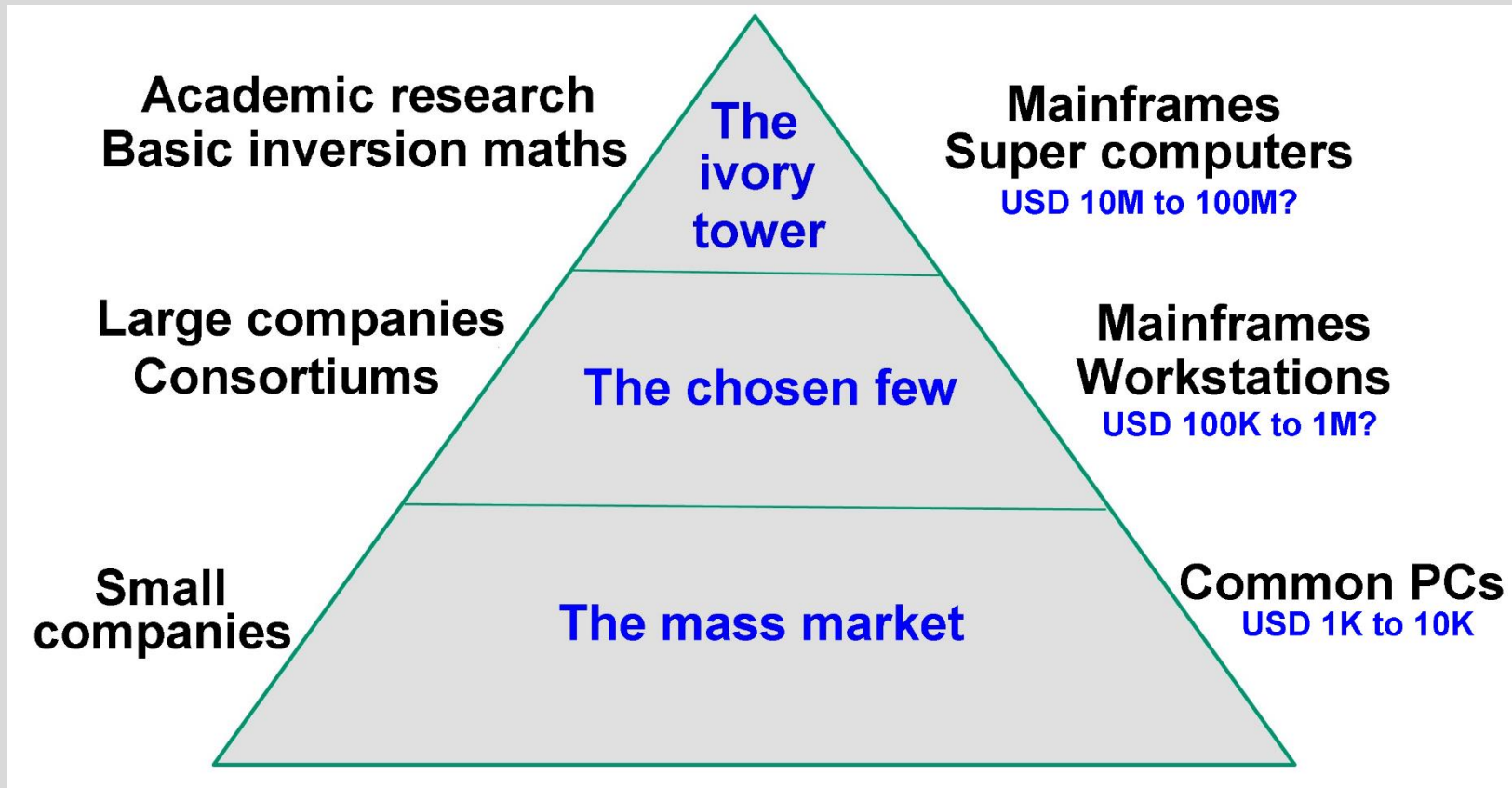
Current electrode of SYSCAL Pro Deep Marine

cable with graphite electrodes



Software social impact : A pyramidal view

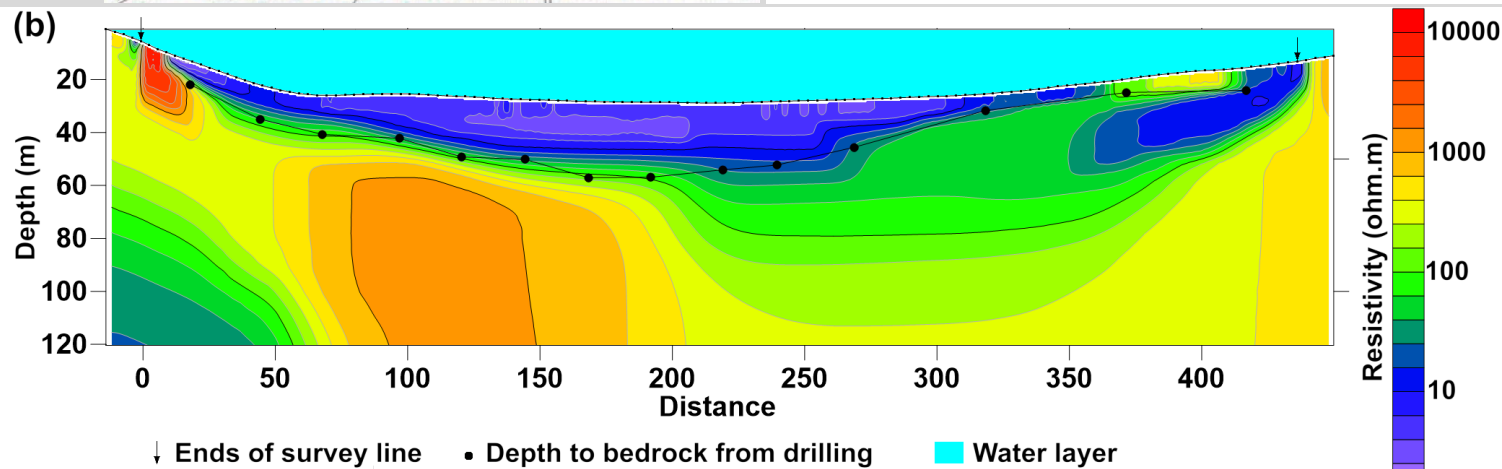
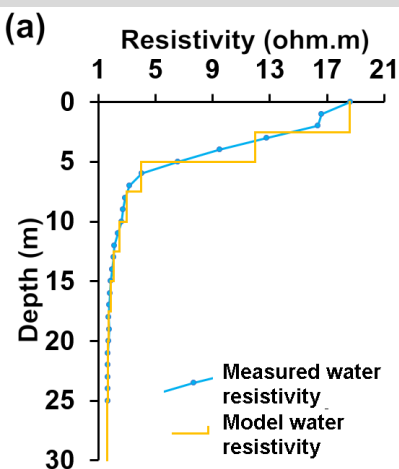
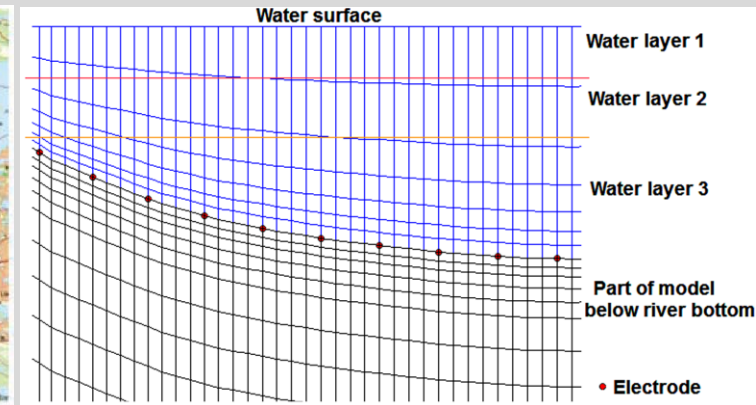
Much of the basic mathematical tools were developed as academic research. The software tools were only initially available to large corporations that funded part of the research.



For small companies, it must run rapidly on common inexpensive PCs. Numerical code optimized for PCs can achieve speedups of 10 to 1000 times. Dey & Morrison 2-D FDF code – speedup of 20 times.

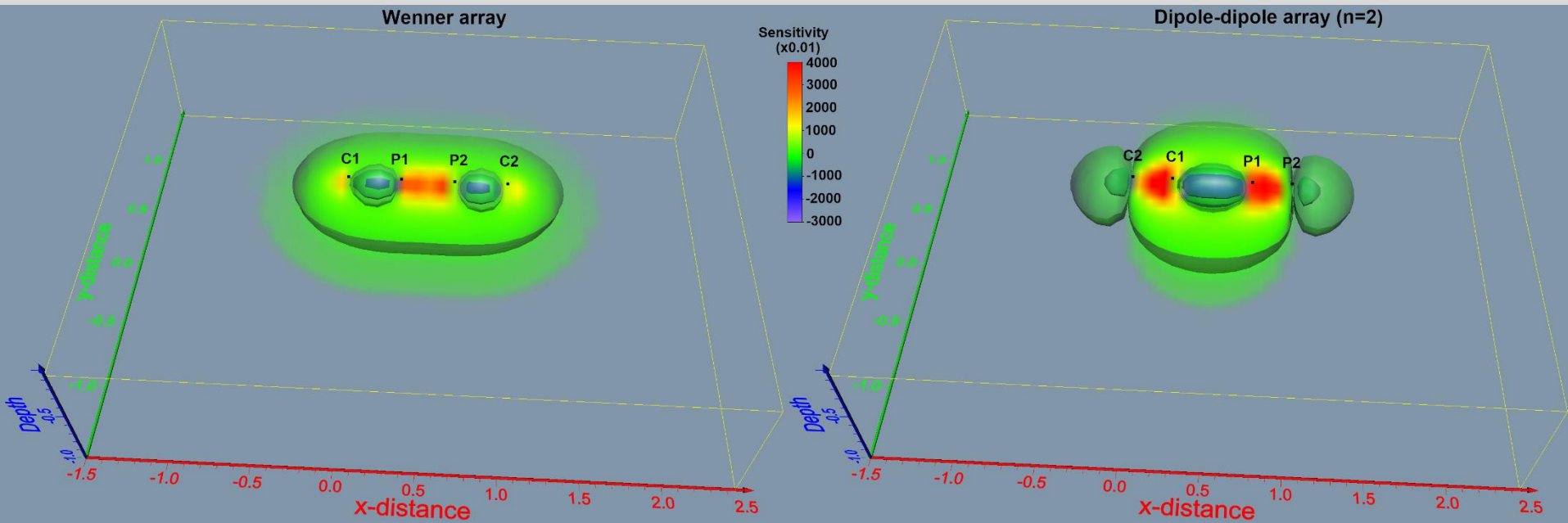
2-D field survey : Below the city by the sea

This survey was conducted along the route of a planned tunnel in part of the sea in downtown Stockholm. Electrodes were laid on the bottom. The pole-dipole array was used. Part of the FEM mesh was used to model the water layer. The shallow low resistivity layer agrees well with drillholes, and a possible fracture zone was detected.



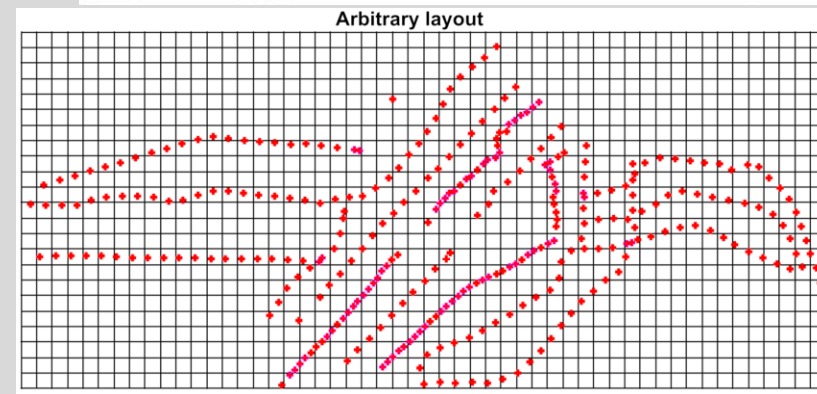
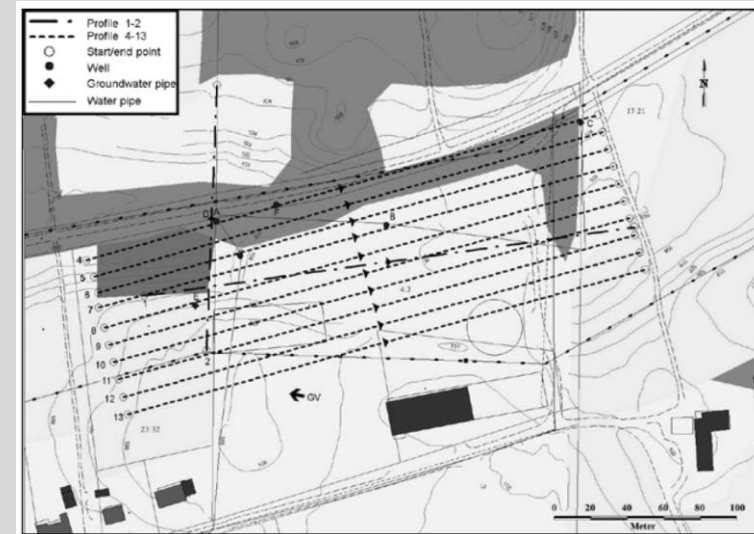
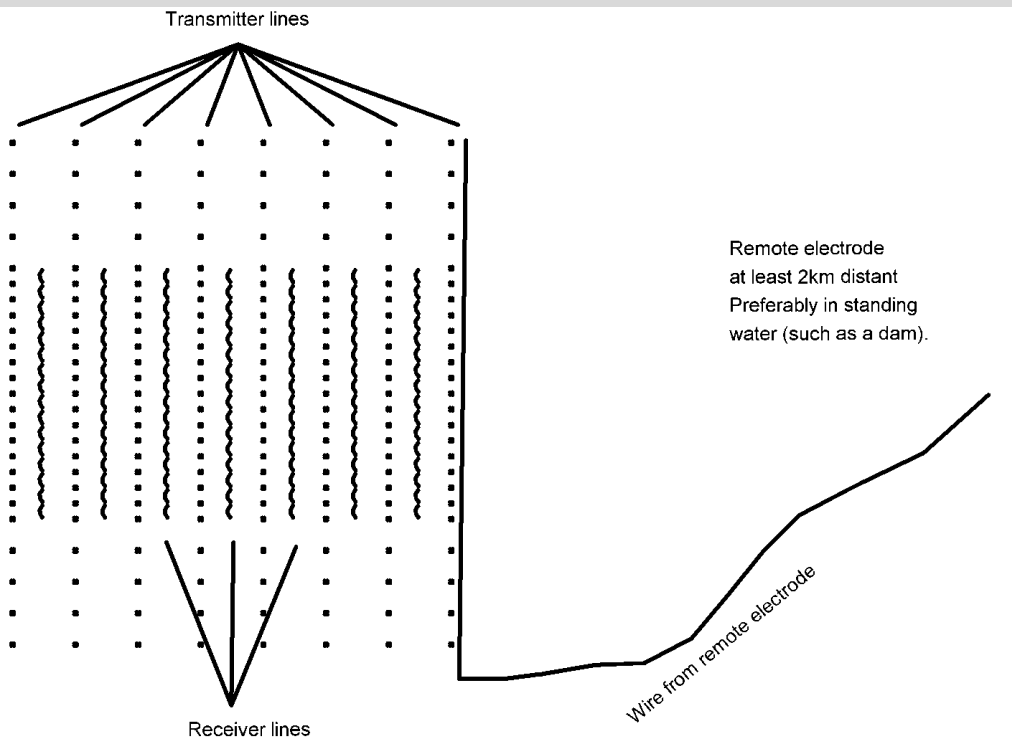
The flaw in the 2-D system

The underlying assumption is that the geology is 2-D, i.e. it does not change in the direction perpendicular to the line. Compared to wave-based techniques such as seismic or GPR, geoelectrical methods are more sensitive to 3-D effects. The severity of the 3-D effects depends on the array type. The high sensitivity zone of the **Wenner** array is elongated along the line of electrodes, thus it is less sensitive to 3-D effects. The sensitivity zone for the **dipole-dipole** array is elongated perpendicular to the array axis, i.e. it is more sensitive to 3-D effects. In very complex environments, a 2-D approach is not good enough.



2000s : Into the real world

The widespread use of 2-D surveys highlighted the problem of 3-D effects in areas with complex geology, particularly in mineral exploration. Some 3-D data are collated from 2-D surveys. More efficient methods to collect the data were devised, such as the offset pole-dipole array. The electrodes can be arranged in a rectangular or irregular pattern.

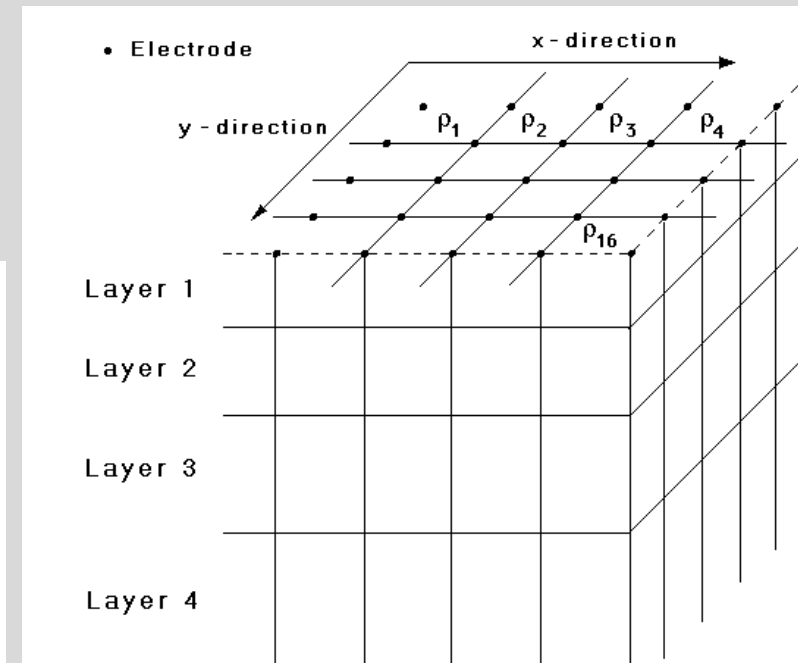
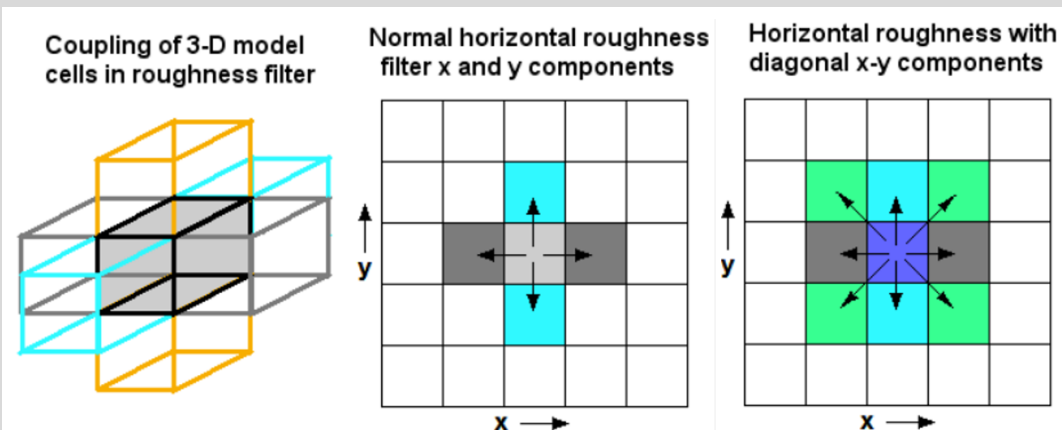


3-D data inversion method

The smoothness-constrained least-squares inversion method optimization method can also be used for 3-D data inversion.

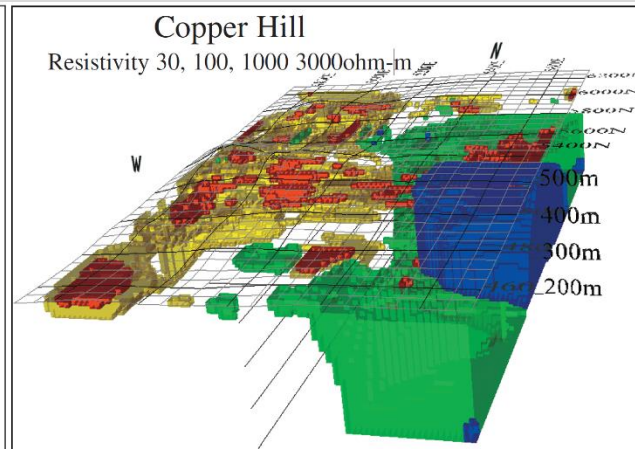
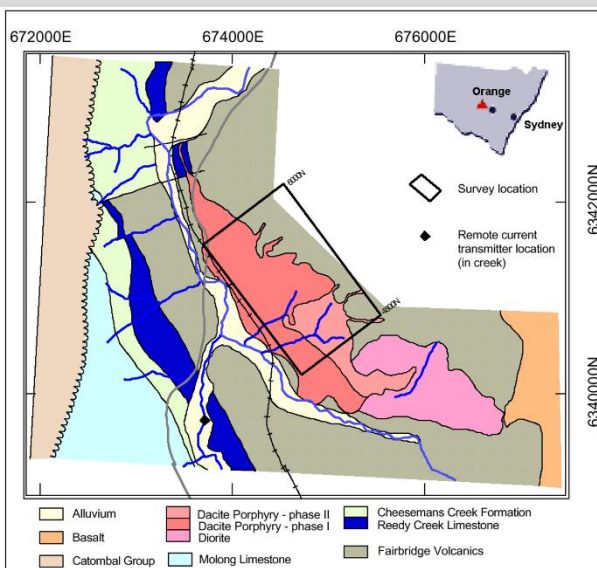
$$[\mathbf{J}_i^T \mathbf{R}_d \mathbf{J}_i + \lambda_i (\mathbf{W}^T \mathbf{R}_m \mathbf{W} + \delta \mathbf{I})] \Delta \mathbf{r}_i = \mathbf{J}_i^T \mathbf{R}_d \mathbf{g}_i - \lambda_i [\mathbf{W}^T \mathbf{R}_m \mathbf{W} + \delta \mathbf{I}] (\mathbf{r}_{i-1} - \mathbf{r}_m)$$

The roughness filter \mathbf{W} has components in the x , y and z directions. Diagonal filter components in the x - y direction are frequently used to reduce artifacts. The subsurface is divided into a number of rectangular prisms. The time taken on a modern multi-core PC ranges from minutes to days depending on the size of the data set.

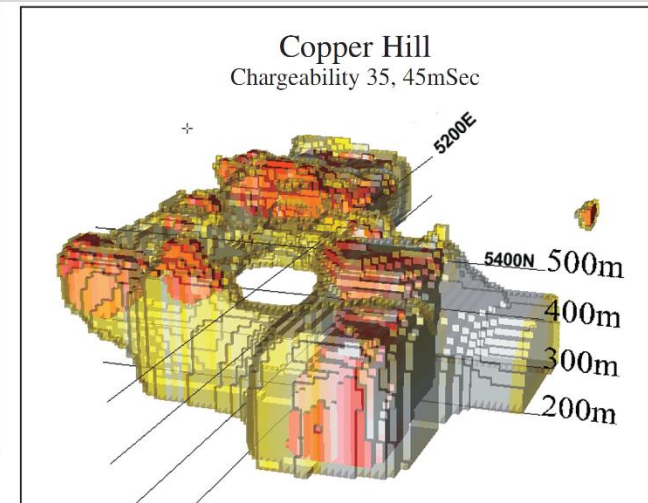


Something old and new

Copper hill is the oldest copper mine in NSW, Australia dating back to 1845. Gold and copper are found in structurally controlled fractures and quartz veins. However, due to the complex geology, large differences in ore grades were found in drill-holes that were less than 200 m apart. In the late 1990s, a 3-D I.P. survey was conducted using the offset pole-dipole layout. The I.P. model shows 2 en-echelon N-S and E-W trends forming an annular zone of high chargeability. The high model I.P. anomalies agrees well with mineralized zones in existing drill-holes.



Resistivity Model. Red low to blue high resistivity. the green and blue areas are coincident with the volcanics.

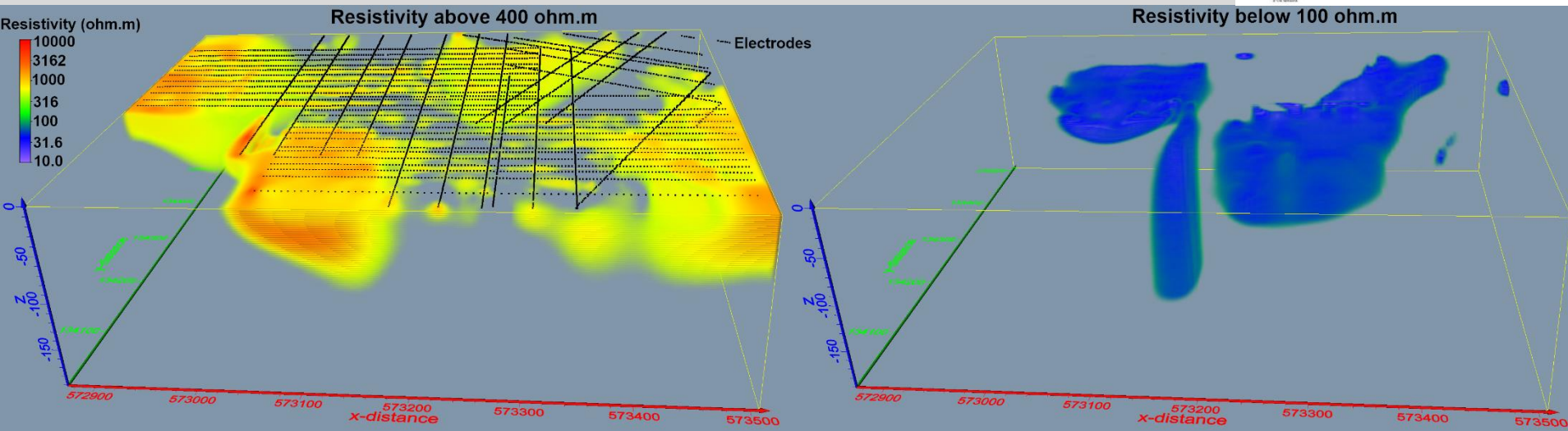
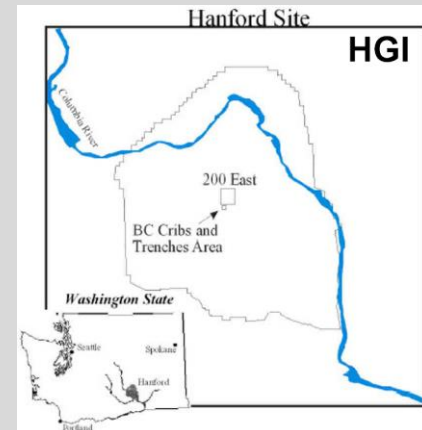


3D Chargeability IP model of Copper Hill with sensitivity controlling the colour saturation.

Toxic legacies

3-D surveys are widely used for landfills and other waste disposal sites. The example below is from the well-known Hanford site. The near-surface high resistivity linear anomalies are concrete cribs. There are two low resistivity zones that are possible leakage zones. The vertical low resistivity anomaly might be a metallic pipe.

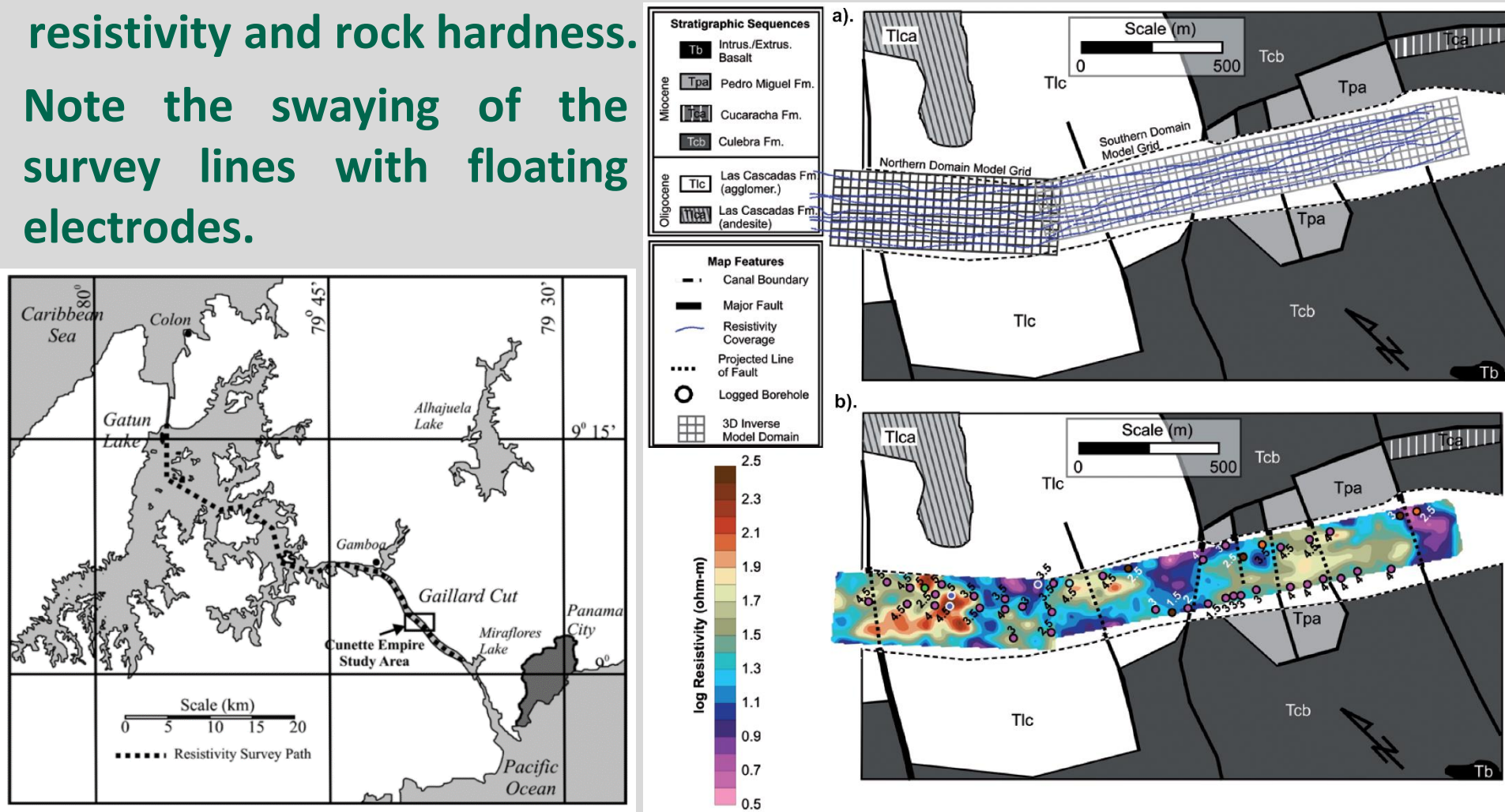
This is a fairly large data set with over 5400 electrodes, 86000 data points, 700000 model cells and a finite-difference mesh with over 16 million nodes. The inversion took 59 hours on a PC with an 18-core CPU and 256GB RAM.



On crooked paths

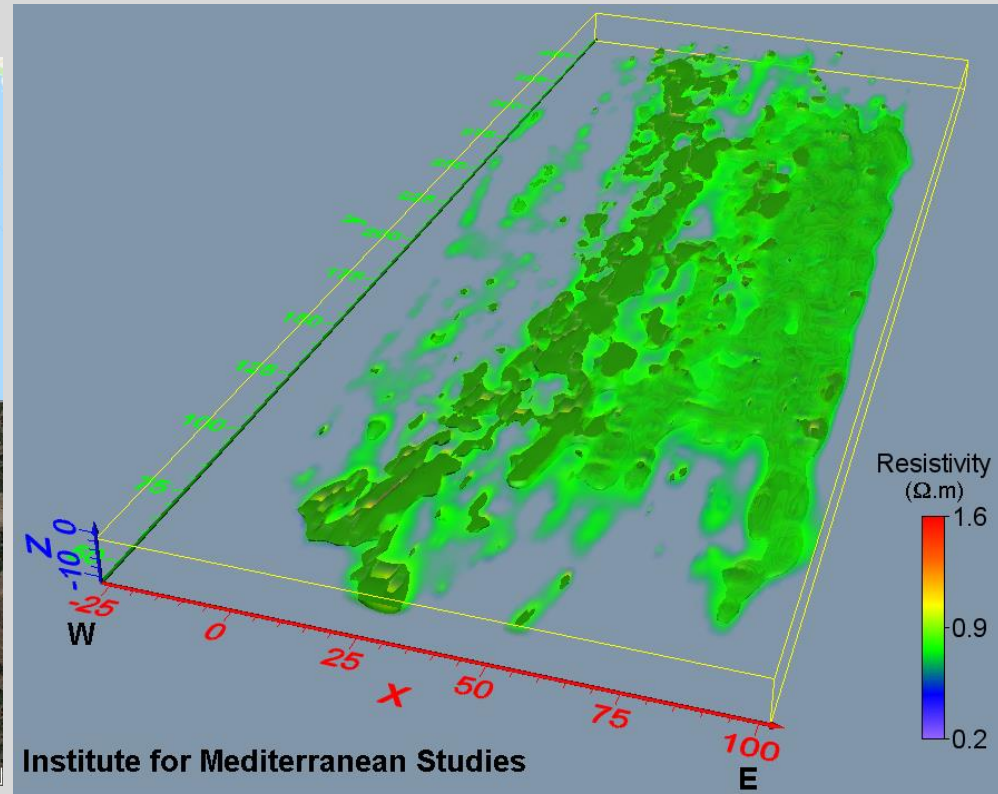
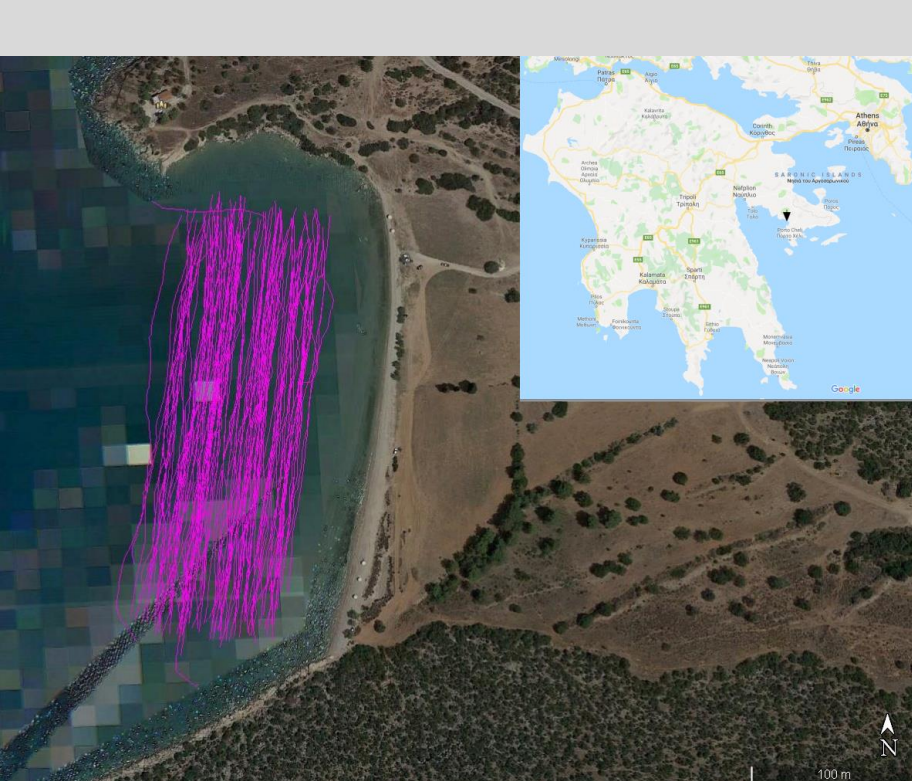
This is from a survey with floating electrodes along the Panama Canal by HGI where sub-parallel lines were collated into a 3-D data set. The resistivity values of a section of the canal about 3 to 4 m below the canal bottom is shown. There is a positive correlation between resistivity and rock hardness.

Note the swaying of the survey lines with floating electrodes.



An ancient city below the waves

This survey was conducted with a streamer pulled along the seabed at the submerged early Bronze Age settlement of Lambayana in eastern Peloponnese about 170 Km southwest of Athens. The average water depth was about 1 meter. The data set had over 215000 electrode positions, 165,000 data points and the FEM mesh used had over 6 million nodes. The shallow high resistivity structures in the western half are submerged urban constructions.



2010s : The best of times

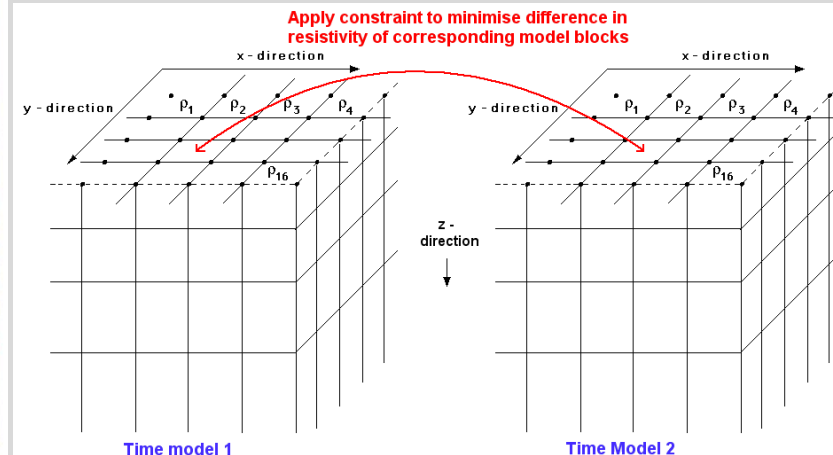
Time-lapse surveys are used to monitor flow of fluids, possible landslides, landfill changes, leakages, aquifer drawdowns. Independent automatic systems that make the measurements at regular intervals and send the data over the Internet are now available, some with solar power. In data inversion, a smoothness-constraint (**M**) is applied across the time models to reduce artifacts.

$$[J_i^T R_d J_i + \lambda_i (W^T R_m W + \delta I + \eta M^T R_t M)] \Delta r_i = J_i^T R_d g_i - \lambda_i [W^T R_m W + \delta I + \eta M^T R_t M] (r_{i-1} - r_m)$$

Italy levee monitoring

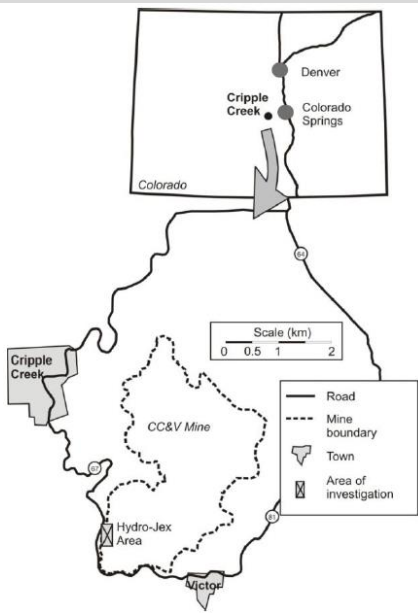


U.K. landslide monitoring

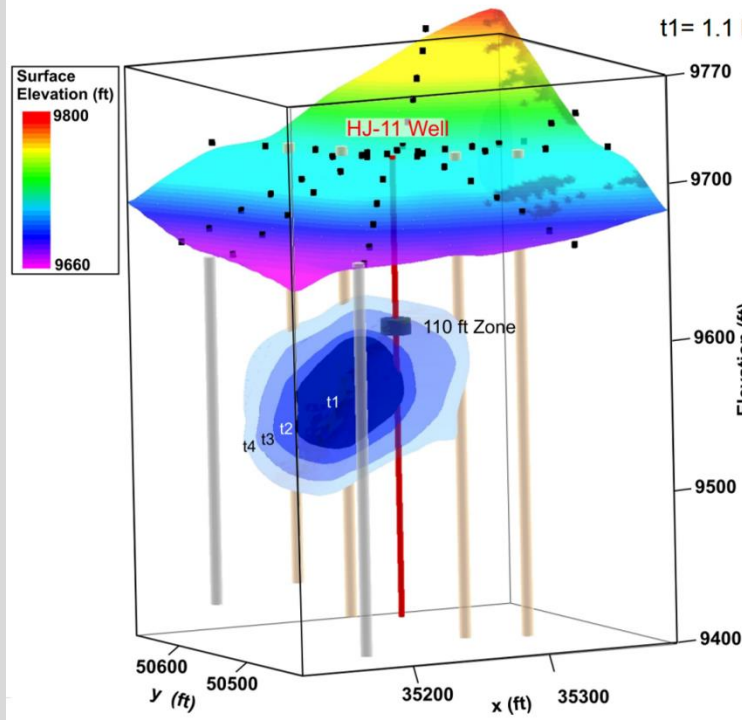


Enhanced gold recovery

A dilute sodium cyanide solution was injected at high pressures into a rock pile to increase the extraction of gold at the Cripple Creek and Victor Gold Mine in Colorado. Resistivity measurements were made with 48 surface electrodes placed along 8 radials, 94 electrodes within six boreholes, and 8 long electrodes using steel-cased injection wells. Below is an example the injection results with the change in the resistivity of -4% that illustrates the migration of the solution.

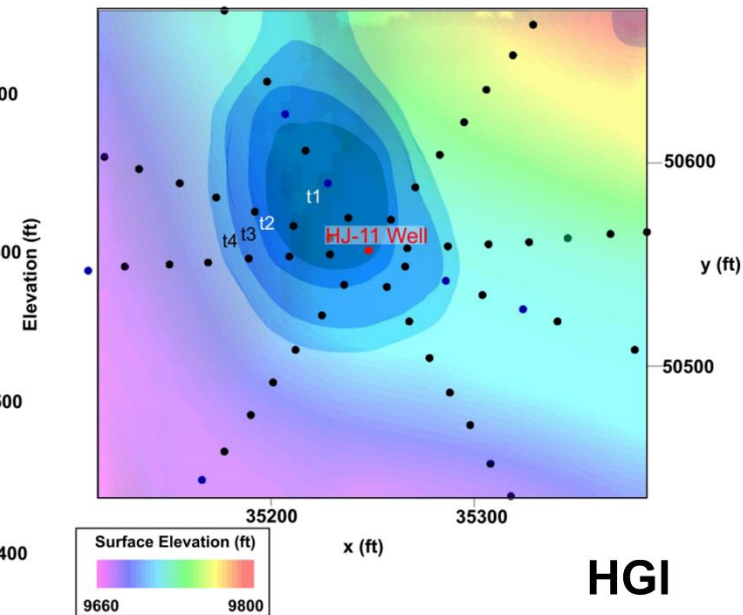


(a) 3D view of inversion results



(b) Overhead view of inversion results

t1= 1.1 hours, t2= 2.4 hours, t3= 3.7 hours, t4= 4.9 hours

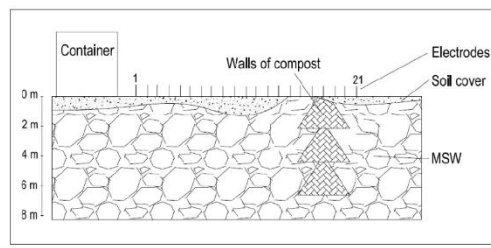
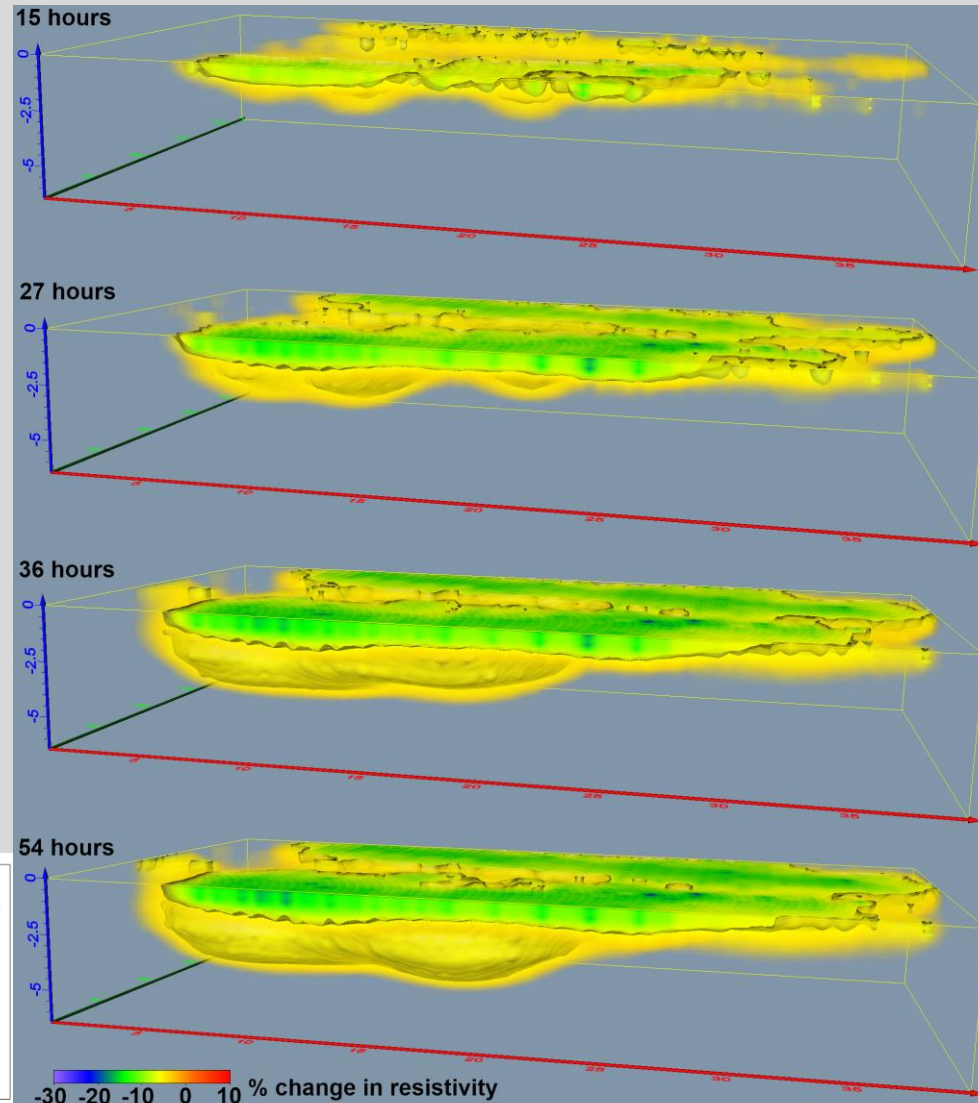


The shape of rainwater

This survey was carried out to map methane gas accumulation in a landfill site in Sweden using 9 parallel 2-D survey lines 2 m apart each with 41 electrodes (1 m spacing) using the pole-dipole array.

Eight sets of measurements were made each day from 2008 to 2011 using an automatic system.

On 2nd July 2001 heavy rainfall occurred lasting about 20 hours. The plots show the migration of the rainwater down a permeable zone after the start of the rainfall. The water table is at 5 m depth.



Summary

1. 1-D surveys are simple to carry out but give models that are not realistic for many areas with complex geology.
2. 2-D electrical surveys have become a standard geophysical technique. It gives the best balance between accuracy and cost in areas with moderately complex geology. The equipment and software are well developed and widely available.
3. 3-D surveys are required to properly resolve areas with complex geology, such as landfill sites and mineral deposits.
4. 4-D surveys is the new frontier where it is necessary to detect temporal changes in the subsurface, such as subsurface water movement and landslide monitoring.

The greatest changes have occurred in the last 30 years, for 1-D to 4-D.

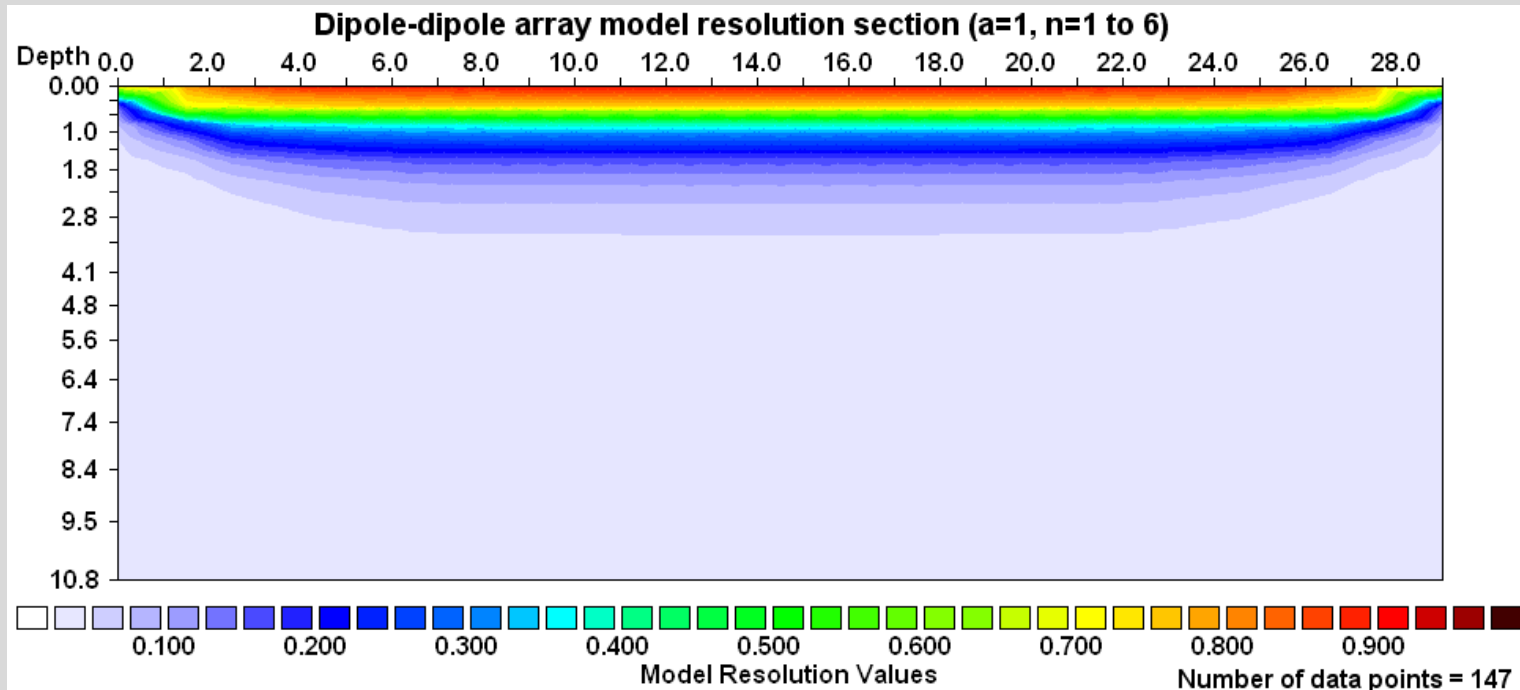
New challenges

- 1). Electrode array optimization, a lesson in numerical optimization**
- 2). Special time-lapse constraints**
- 3). Vector arrays**
- 4). Structured, unstructured and semi-structures meshes**
- 5). Affordable tech for emerging countries**

The electrode array optimization problem

Problem : If the number of electrodes and measurements are specified, what are the 'best' arrays to use to get the maximum 'resolution' of the subsurface? From least-squares inversion theory, the resolution matrix R is given by :- $R=BA$, where $B=(J^T J + \lambda F)^{-1}$, $A=J^T J$.

J =Jacobian matrix, λ =damping factor, F =regularization matrix. The diagonal elements R_{ii} give the model cells resolution. Example plot of resolution values for dipole-dipole array with 30 electrodes. Resolution values range from 0.0 to 1.0. Cutoff value ≈ 0.05 .



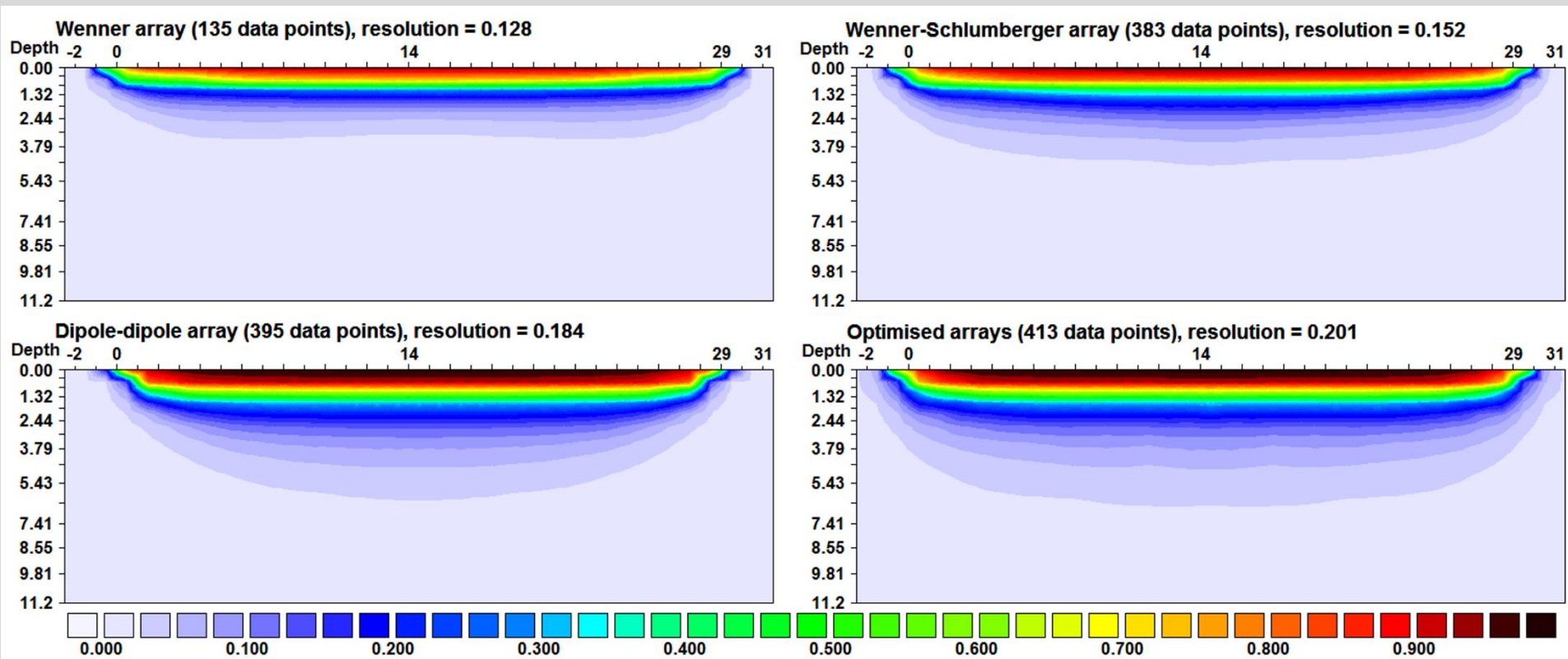
Resolution plots of different arrays

Maximum survey depth with cutoff resolution value 0.05.

Wenner ≈ 3.0 m, Wenner-Schlumberger ≈ 4.0 m with relatively flat zone of higher resolution.

Dipole-dipole (a=1 to 3, n=1 to 6) ≈ 6 m, lower resolution at ends

Optimized arrays ≈ 7.0 m with wider zone of higher resolution

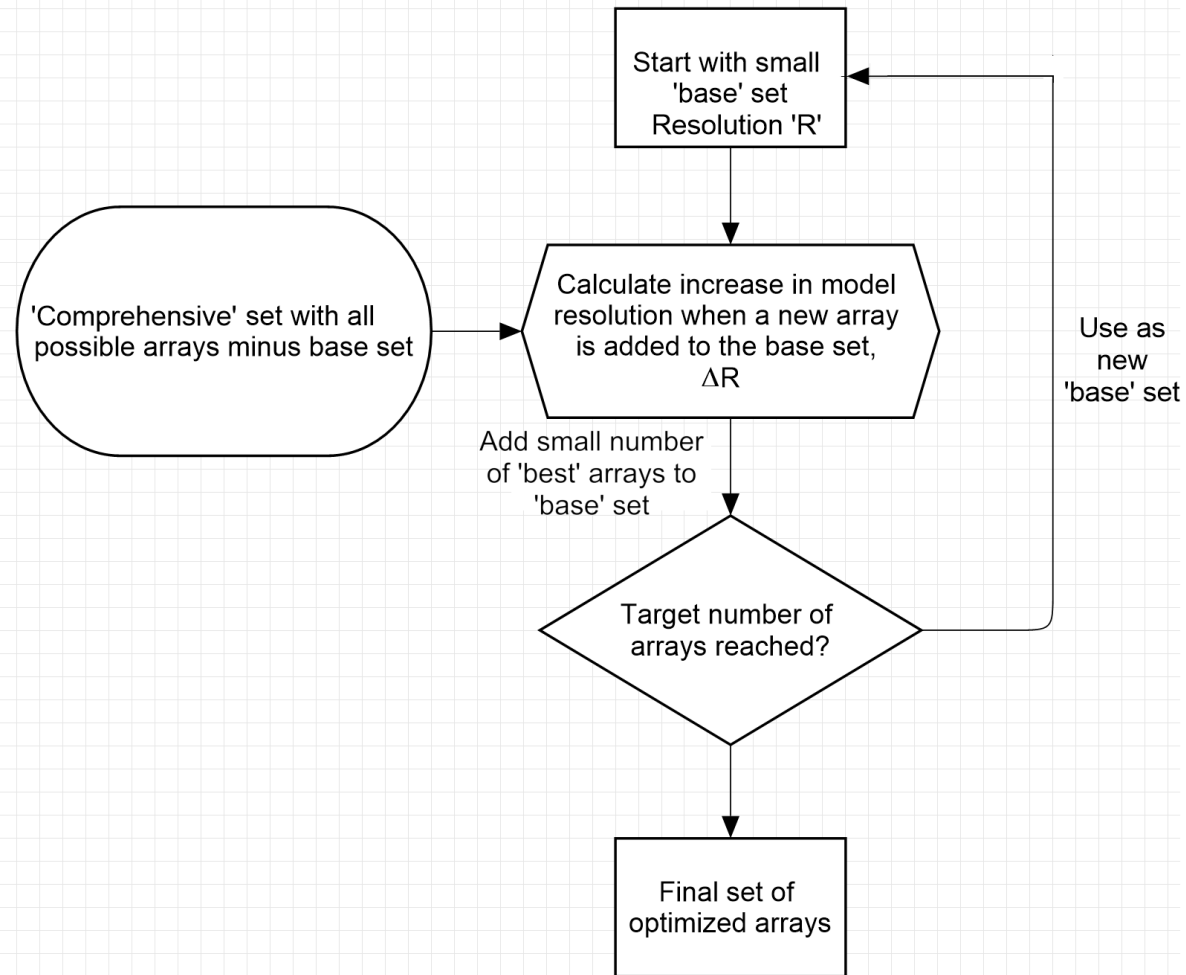


Optimized array generator algorithm

A survey line with E electrodes has $N = E(E-1)(E-2)(E-3)/8$ possible 4-electrode arrays. Reduced by excluding arrays with large geometric factors and those that are unstable (C1-P1-C2-P2). A line with 30 electrodes has a 'comprehensive set' of 51283 unique arrays.

The starting 'base' set can be dipole-dipole arrays with $a=1$, $n=1$ to 6.

The important numerical calculation is in find the change in the model resolution, ΔR , when one new array is added to the base set.



Improving the maths and linear algebra

The Sherman-Morrison update is used to calculate the new A and B matrices when 1 new array is added to the base set (4 steps).

Calculate $A_{b+1} = A_b + gg^T$ and $B_{b+1} = B_b - zz^T / (1 + \mu)$, with $z = B_b g$ and $\mu = g \cdot z$

Then find $R_{b+1} = B_{b+1} A_{b+1}$, finally $\Delta R_{b+1} = R_{b+1} - R_b$

g is sensitivity vector for the test array. Repeat for 51000+ test arrays.

Fast method

Simplify to 1 step, $\Delta R_{b+1} = z(g^T - y^T) / (1 + \mu)$, with $y = A_b g$, $z = B_b g$, $\mu = g \cdot z$

Final calculation only involves vectors. Main work is matrix-vector multiplications $z = B_b g$ and $y = A_b g$ for each test array.

Calculate many test arrays at a single time, eg. $G = g_1 g_2 \dots g_{100}$ and use fast BLAS GEMM matrix-matrix multiplication routine, eg $Z = B_b G$. Greatly reduce memory access for A_b and B_b .

Overcoming the bottlenecks

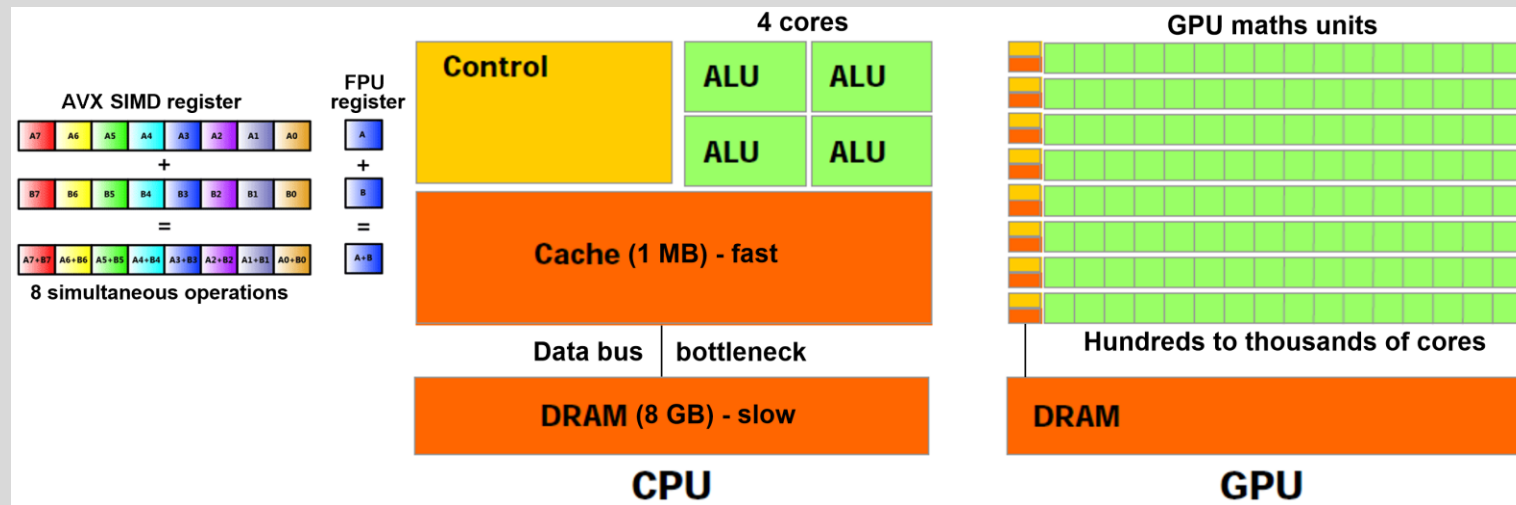
Better Maths – Simplify equations for ΔR to minimize memory transfers from slow RAM to fast CPU. Main operation BLAS GEMM.

Maximize CPU – Besides using multiple CPU cores, leverage the SIMD registers (4 to 16) within each core.

Use Graphics Card – For matrix-matrix operations, offload to GPU which have 100s to 1000s of cores. Nvidia CUDA library.

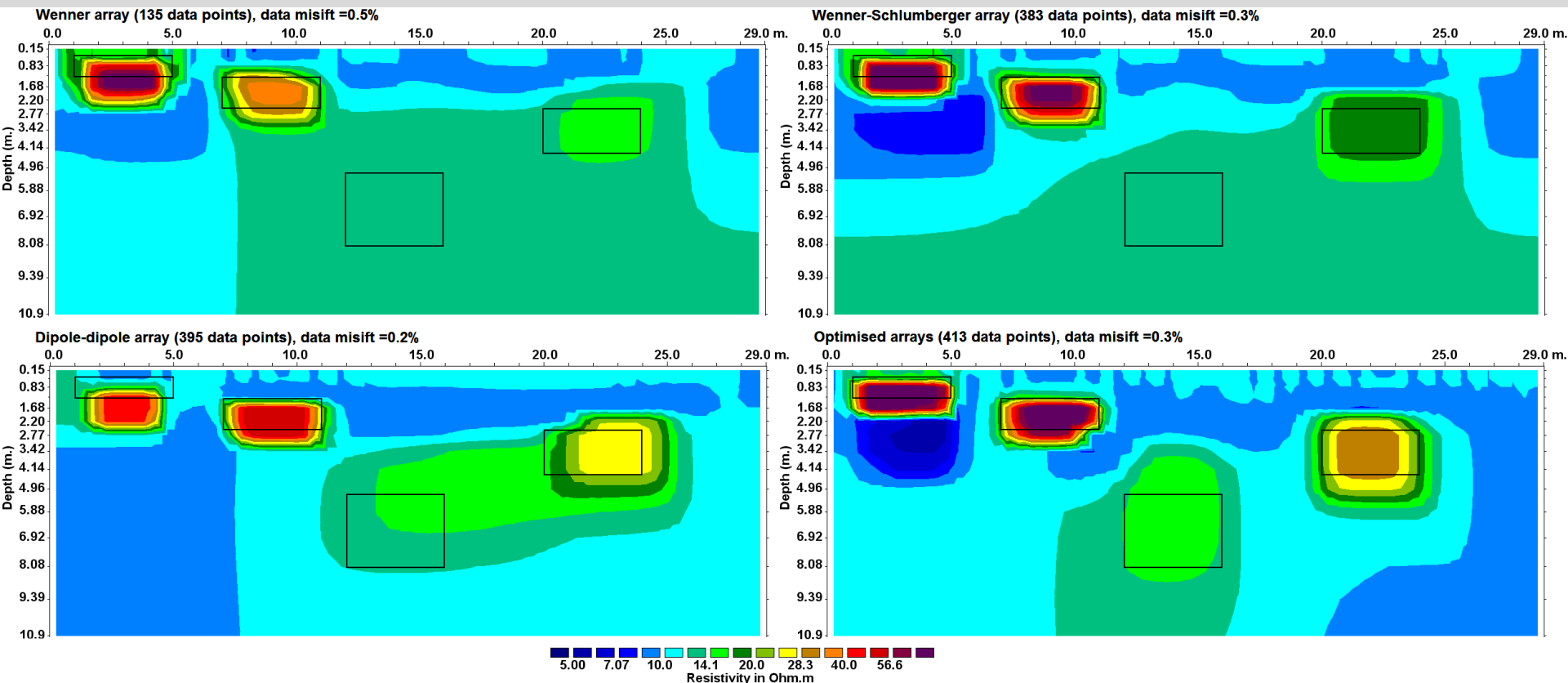
Work Smarter - Instead of calculating for 51000 C1-C2-P1-P2 arrays (A.g), calculate for 435 C-P pairs and add up contributions from 4 C-P pairs ($g_1+g_2+g_3+g_4$) to reconstruct values for the 4-electrode array.

Calculation
time reduced
from 6 hours
to 10 secs :
2000 times
faster !



Example of resolution improvement

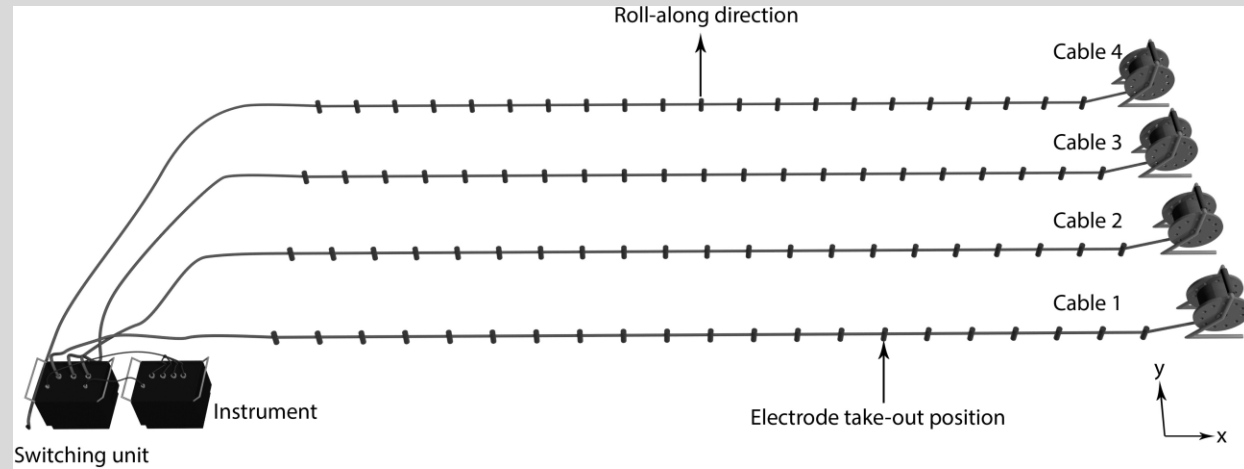
The test model has 4 rectangular blocks of $100\ \Omega\cdot\text{m}$ in a $10\ \Omega\cdot\text{m}$ medium. The top 2 blocks are well resolved by all the arrays. The 3rd block is poorly resolved by the Wenner array but well resolved by the dipole-dipole array. The dipole-dipole array is unable to separate the 3rd and 4th blocks, but they are resolved by the optimized arrays.



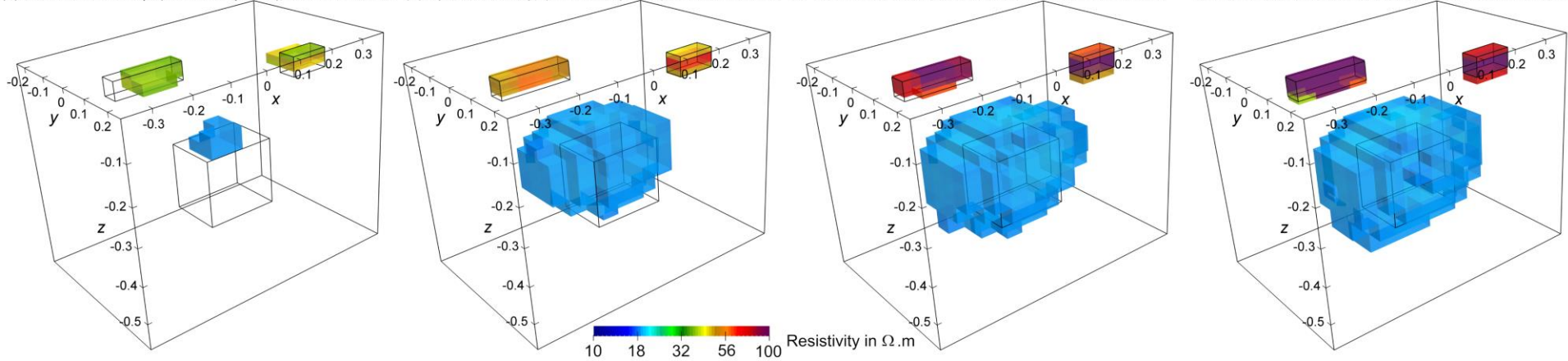
3-D optimized arrays

The top figure shows a field survey where 3 cables, each with 21 electrodes, can be accessed at a single time. A roll-along method is used to cover a wider area. Optimized arrays were generated for this arrangement, and compared with conventional arrays (combined dipole-dipole and Wenner-Schl).

Results from a tank experiment with 3 plastic blocks in water are shown.

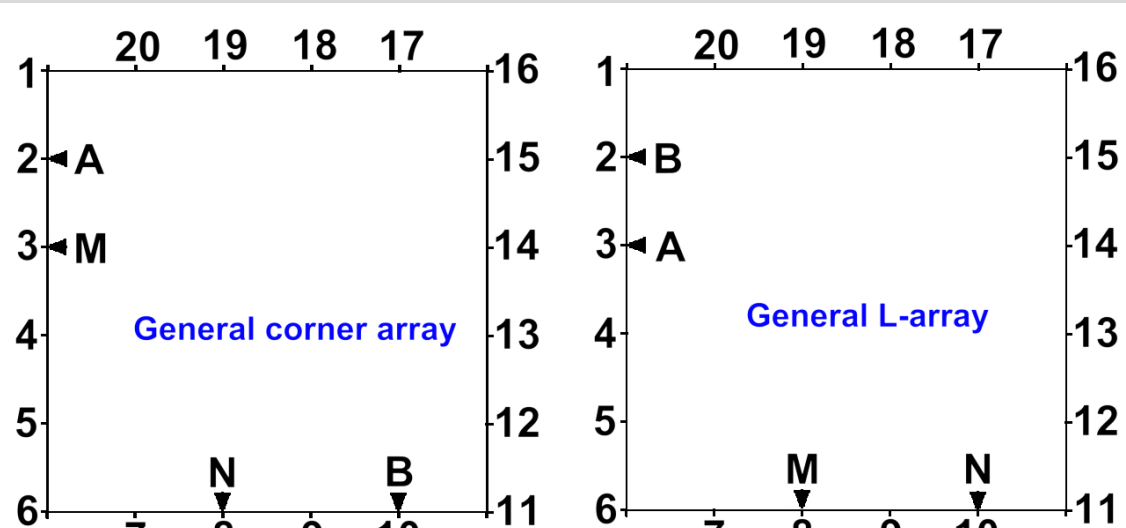
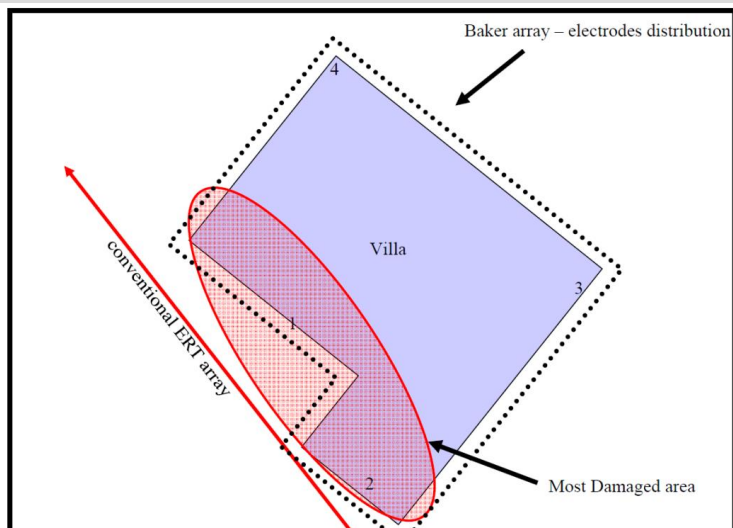


(a) Conventional arrays (1414 data points), data misfit 0.5% (b) Optimized arrays (1416 data points), data misfit 0.7% (c) Optimized arrays (2500 data points), data misfit 0.6% (d) Optimized arrays (5001 data points), data misfit 0.6%



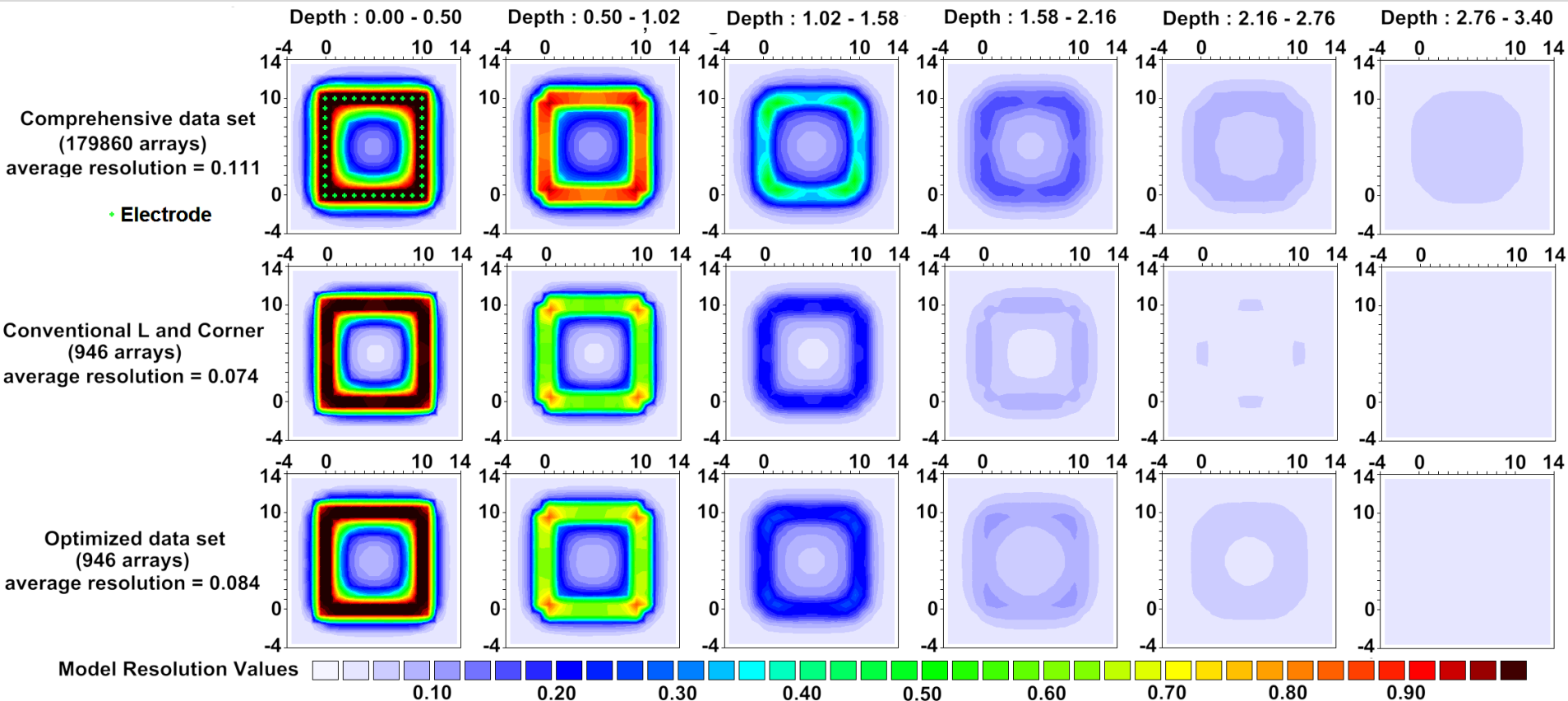
Perimeter surveys

Surface of some built-up areas are paved, and it is not possible to use normal implanted electrodes. The electrodes are confined to the perimeter of the survey area. Arrays that have been used, such as the 'Baker' and "L & corner' arrays, are based on heuristic rules designed for perimeters with sharp corners. The resolution based array optimization method provides a numerical criteria to assess the effectiveness of the different arrays.



Perimeter surveys – resolution tests

We compare the resolution of the ‘L & Corner’ arrays with the optimized arrays for a square perimeter with 40 electrodes. The comprehensive data set has significant resolution until the 6th layer, while the smaller optimized data set reaches until the 5th layer. The optimized data set has better resolution compared to the ‘L & Corner’ arrays towards the center and in the deeper layers.

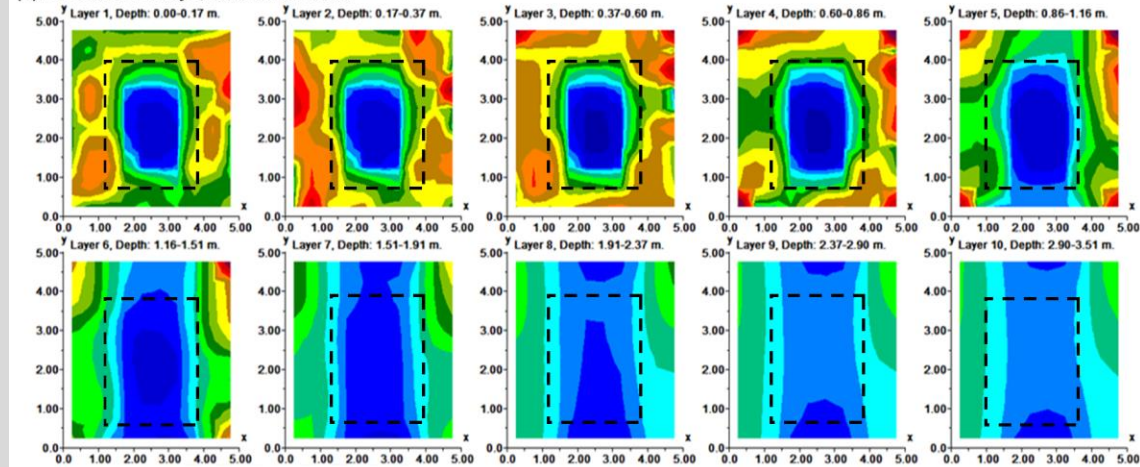


Perimeter survey – field test

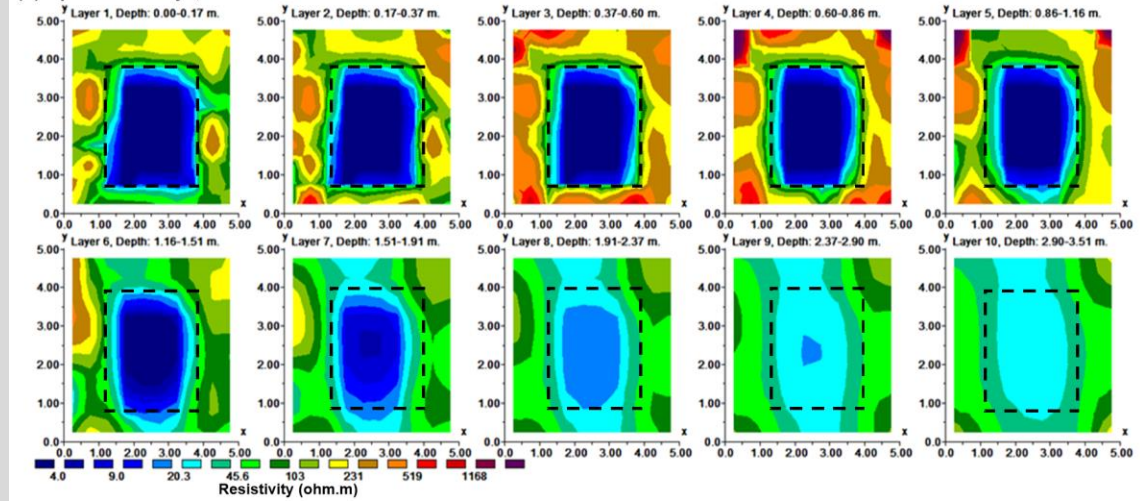
The field test was conducted with the electrode surrounding a metal grating on the surface using electrodes 0.5 m apart. The optimized arrays show the lateral extent of the grating more accurately. Surveys with electrodes confined to the perimeter have poor vertical resolution.

The ‘L & Corner’ arrays model has the anomaly extending to the deepest model layer, while the optimized arrays model cuts it off about 2 meters depth.

(a) L & Corner arrays, data misfit 6.4%



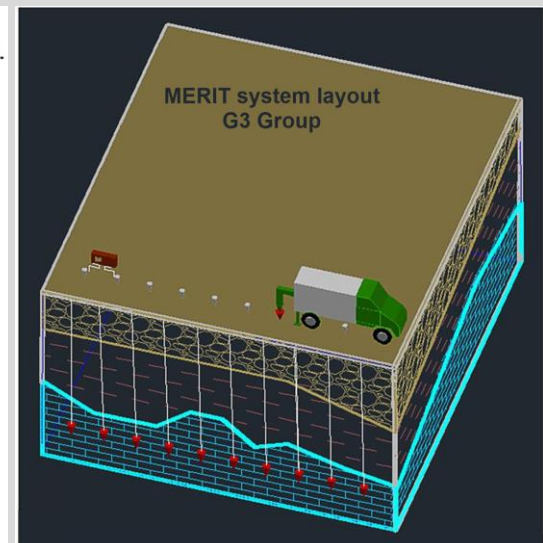
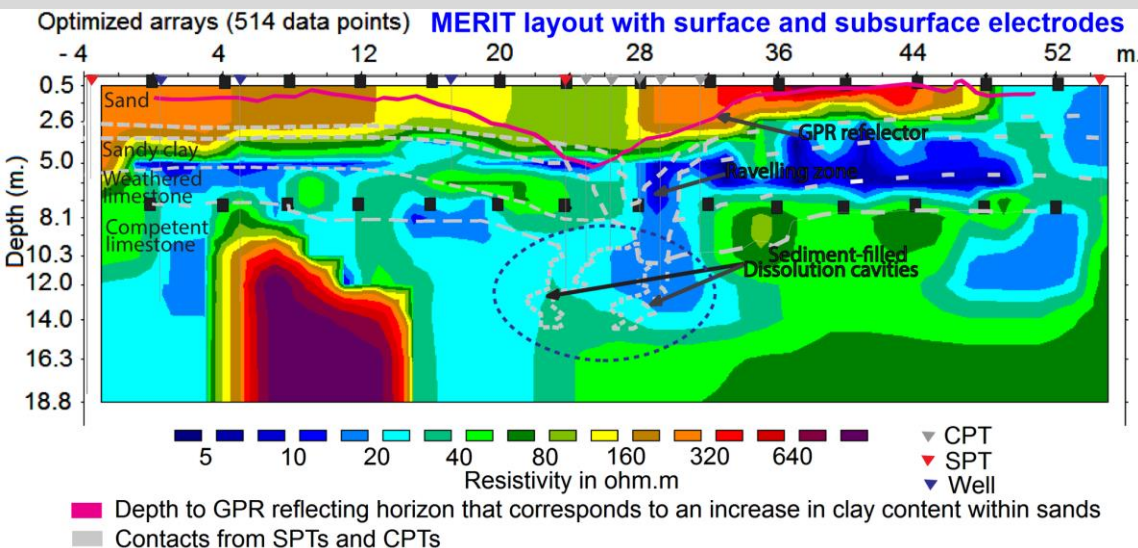
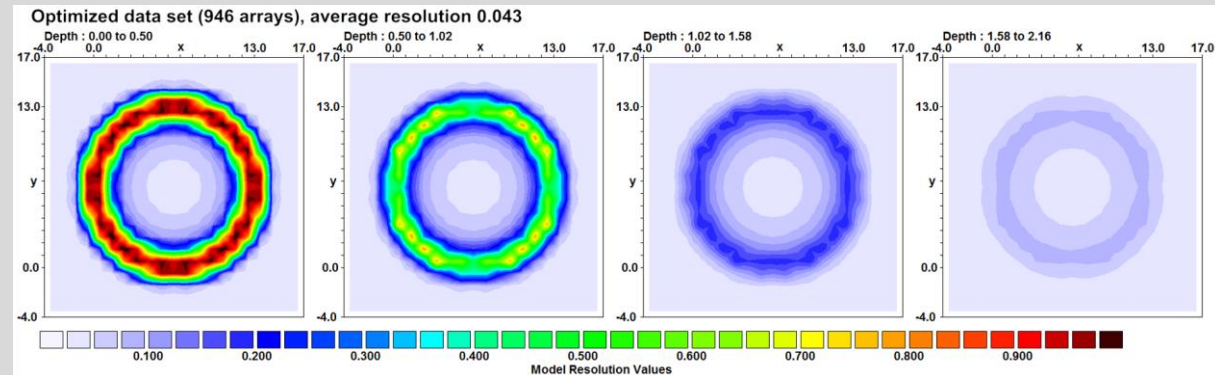
(b) Optimized arrays, data misfit 5.8%



Other applications of optimized arrays

As the model resolution can be calculated for any survey layout, the optimized array method can be used for situations where there are no heuristic rules, such as non-rectangular perimeters. It can be used for vertical boreholes, combination of surface and subsurface rows of electrodes.

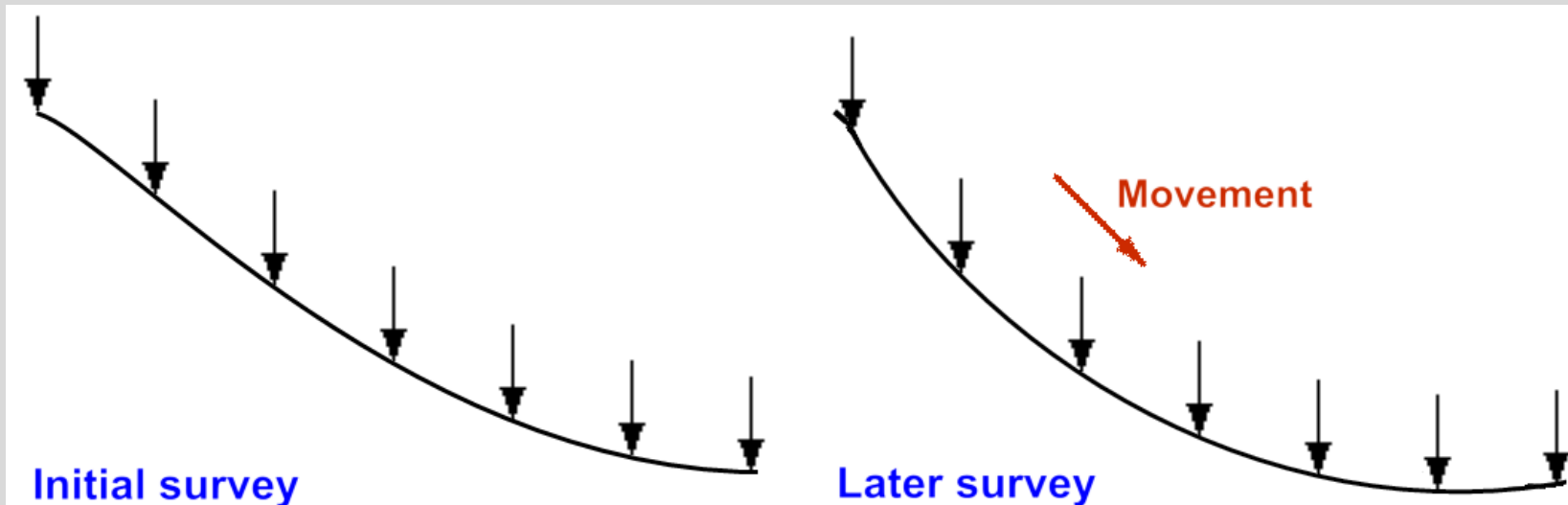
Additional constraints such as noise reduction and focussed regions can be added.



Landslide 4-D survey : On shifting sands

Landslides are often associated with groundwater changes. A problem occurs when the electrodes positions change with time, and the positions are not known for some data sets. What we have :-

- 1). Positions of the electrodes are measured at the start, but electrode positions as well as subsurface resistivity change with time. Both resistivity and electrode positions have to be estimated from apparent resistivity data alone.
- 2). The direction of movement is unidirectional – downslope. Amount of movement variable, depending on slope and geology.



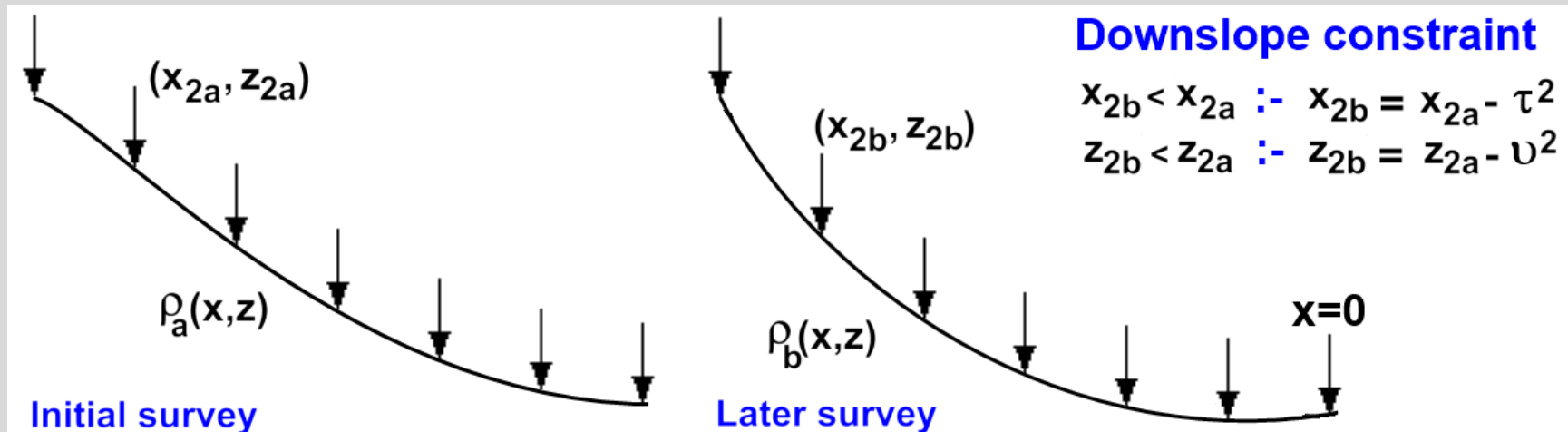
Modified 4-D inversion method

The modified least-squares includes the (x,z) positions for 2-D line.

$$[G_i^T R_d G_i + \lambda_i (V^T R_m V + \delta I + \eta M^T R_t M)] \Delta q_i = G_i^T R_d g_i - \lambda_i [V^T R_m V + \delta I + \eta M^T R_t M] (q_{i-1} - q_m)$$

The modified parameter vector $q=(r \ x \ z)$ includes the positions of the electrodes. The new Jacobian $G=(J \ X \ Z)$ has X and Z that are the partial derivative wrt the (x,y) electrode positions. The roughness filter term $V = (W \ \alpha W_x \ \beta W_z)$ has W_x and W_z that are the roughness filters for x and z with damping factors α and β .

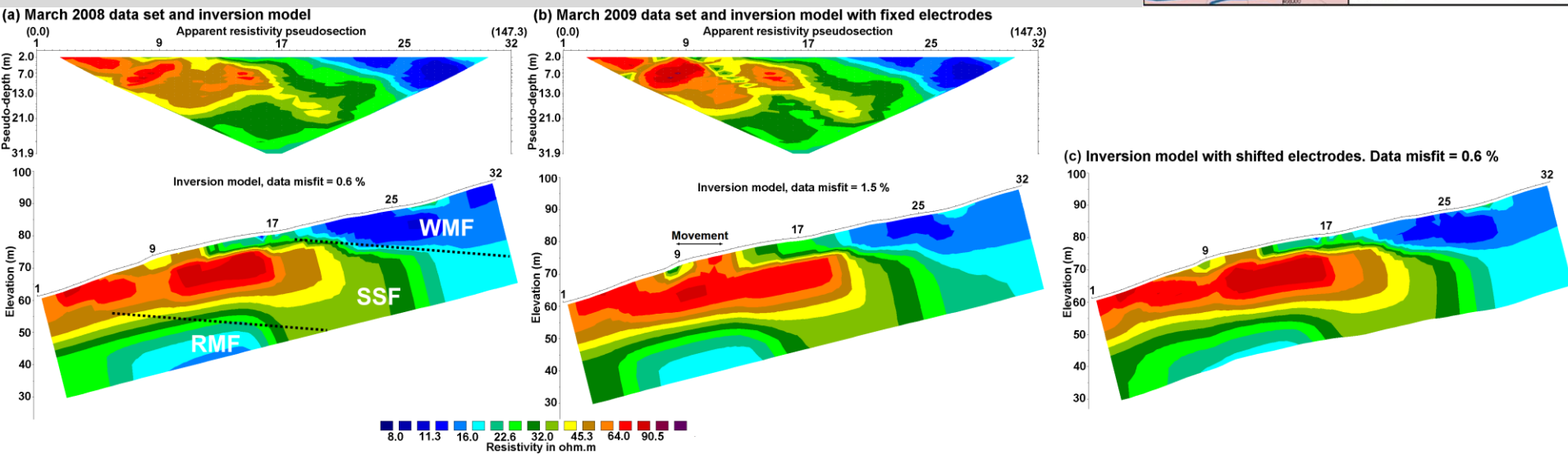
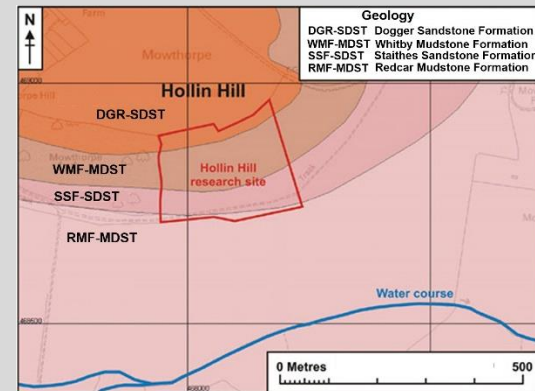
The downslope constraint is set using the method of transformations, eg. the variable x is replaced by τ .



Hollin Hill landslide example

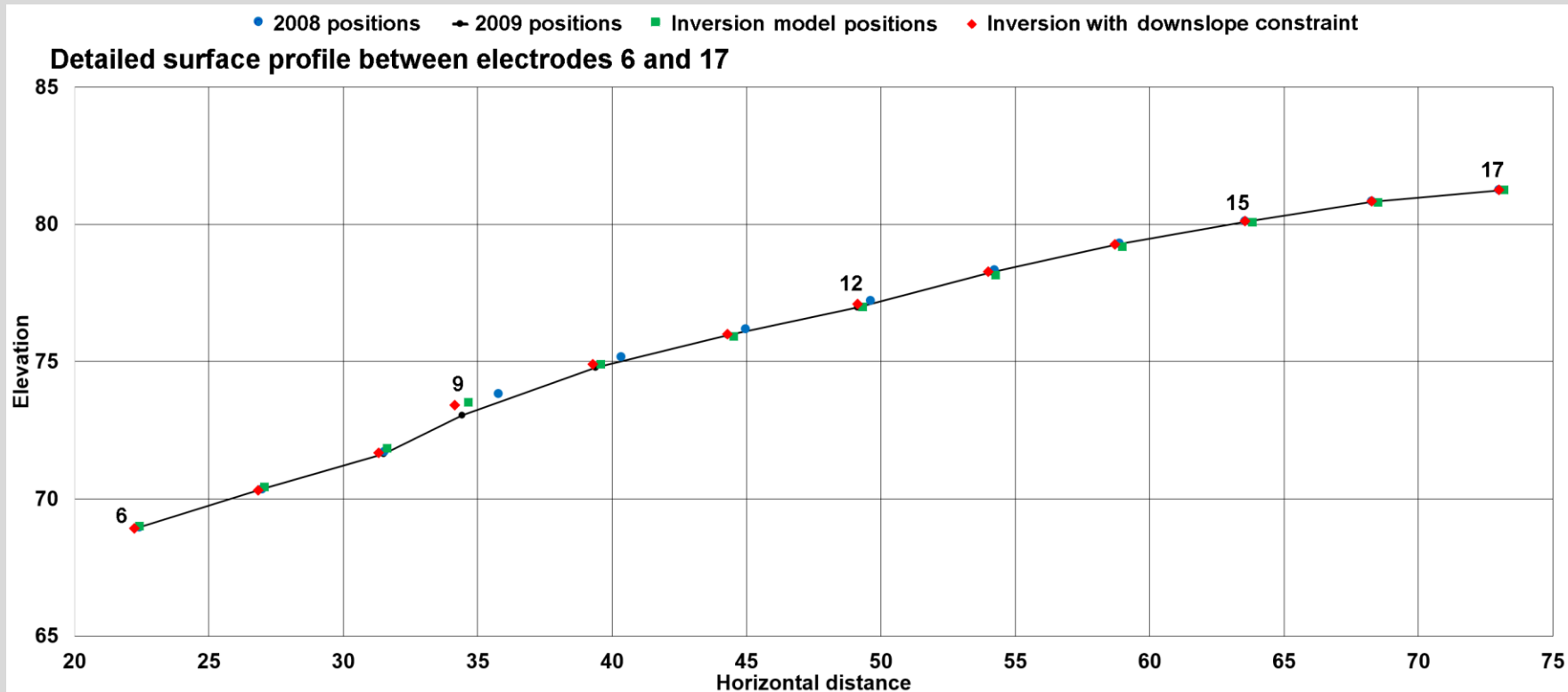
The data is from surveys in March 2008 and March 2009 at the BGS Hollin Hill test site. Landslides occur at the mudstone formation (WMF) above a sandstone (SSF) formation on a slope. The inversion was first carried out using fixed electrode positions from the March 2008 survey.

There are significant near surface artifacts in the 2009 model due to movements near electrode 9. The artifacts are removed when the electrodes are allowed to shift in the inversion.



Constrained inversion for shifting electrodes

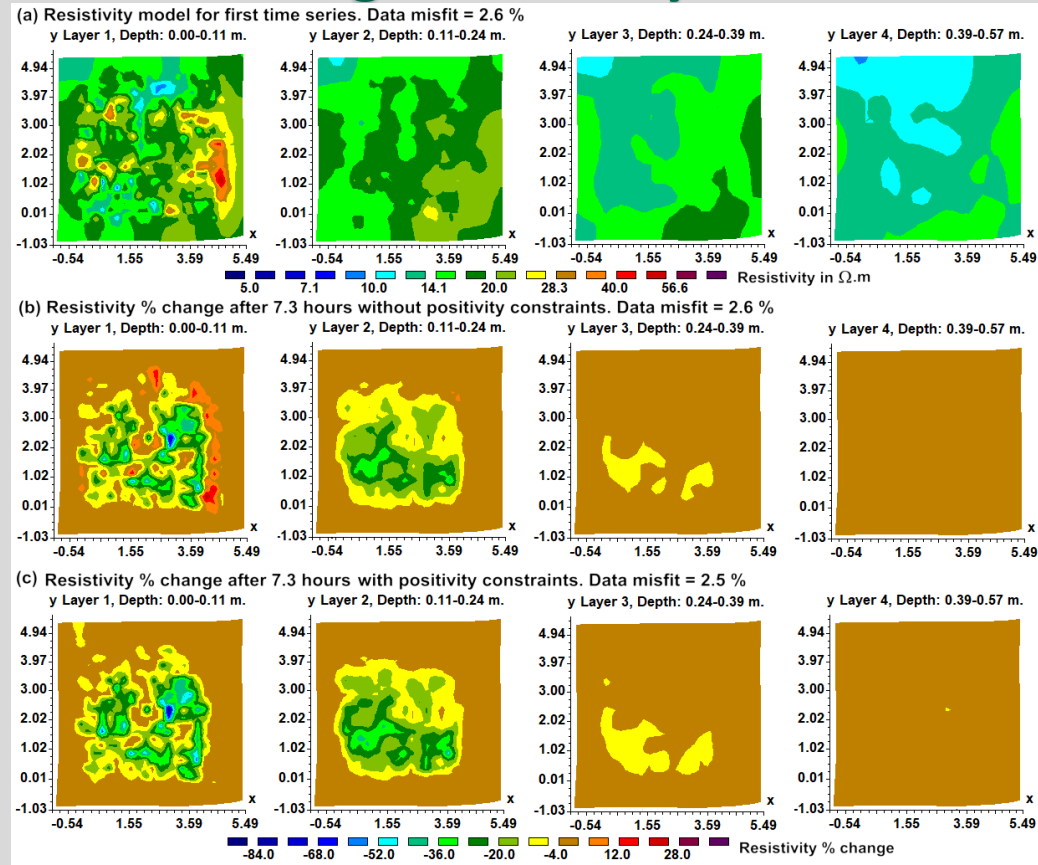
The inverse model **2009 electrodes profile** without the downslope constraint shows a slight shift upwards at positions 15 to 17 compared to the **2008 positions**. To remove this artifact, the method of transformations is used so that the electrodes only move downwards. The RMS difference between the estimated electrode positions and the **true 2009 positions** is reduced from 0.2 to 0.1 m with the **downslope constraint**.



Directional time-lapse resistivity inversion

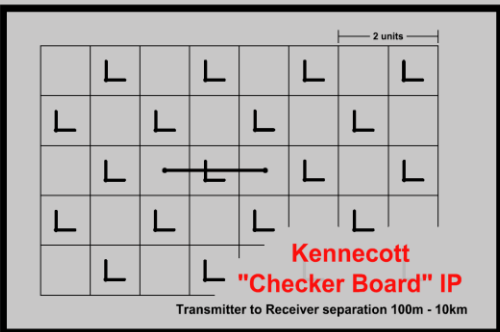
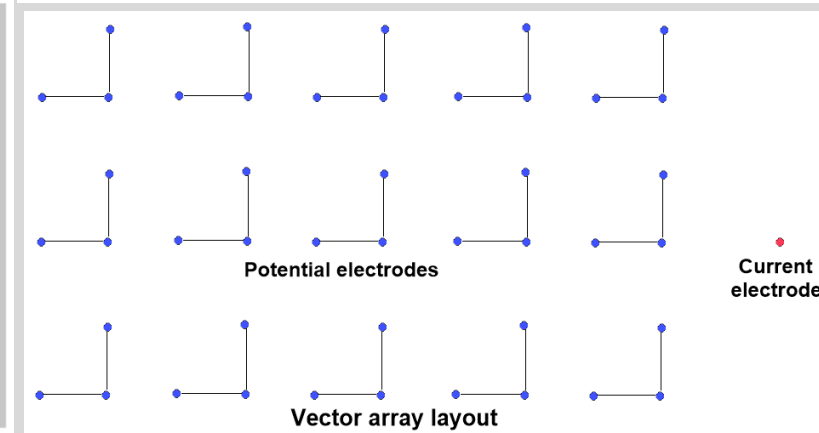
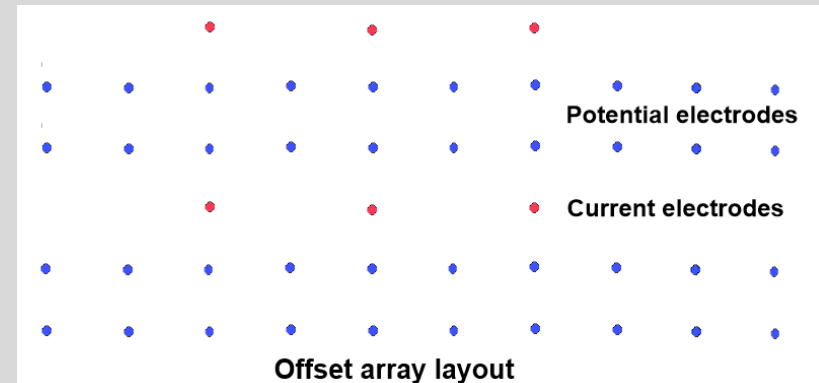
In some cases, it is known that the resistivity should only decrease (or increase) with time. Results are shown below from an experiment at the BGS Hollin Hill test site where saline water was sprinkled on the ground surface to study the effect of fissures on hydrological processes. The model from the standard 4-D inversion method shows large increases with time near the shallow high-resistivity zones.

The artifacts are removed using the method of transformations to ensure that the resistivity only decreases with time.

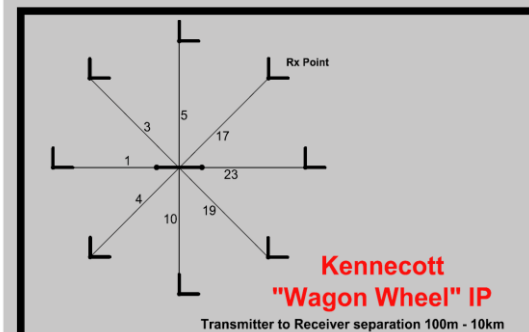


Surveys with vector arrays

Deep I.P. surveys for mineral exploration require a different class of instruments and field techniques. Over the last 25 years, different methods have been devised to reduce the survey costs and time. One system is the offset type of survey. Another system uses the potential electrodes arranged as triplets with the two dipoles at right angles (Zonge 'Kennecott wagon wheel, checker board', Quantum, SJ Geophysics Volterra, Iris FullWaver).



Zonge (1994)



Data from vector arrays

Each potential station has 3 electrodes, one common P1 (M) and 2 separate P2 (N). Measurements are made C1-P1-P2_a and C2-P1-P2_b.

Normal method : Treat them as 2 separate apparent resistivity values. Problem :- one potential pair (eg. P1-P2_b) might be almost perpendicular to current electrode C1, very low potential with extremely high geometric factor, and very sensitive to noise.

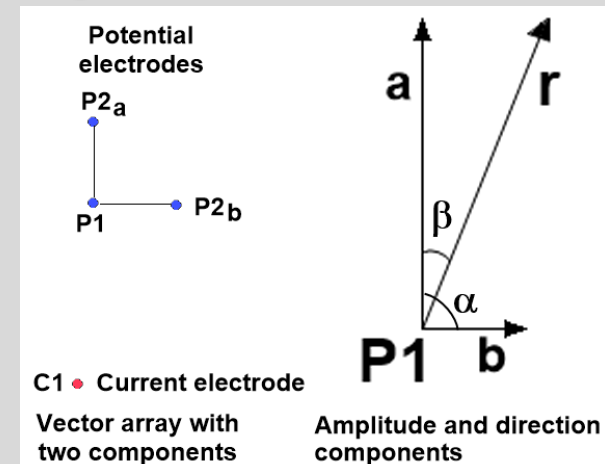
Possible solution : Calculate amplitude (r) and direction (β). The amplitude 'r' will always have a higher potential than individual components 'a' and 'b', i.e. smaller geometric factor and less sensitive to noise. The direction (β) has a finite range of values.

Amplitude : $r^2 = a^2 + b^2 + 2ab.\cos(\alpha)$

Geometric factors : $G_a = 2\pi/p$, $G_b = 2\pi/q$

Amplitude geometric factor, $G_r = 2\pi/s$

$s^2 = p^2 + q^2 + 2pq.\cos(\alpha)$



Vector arrays field survey layout example

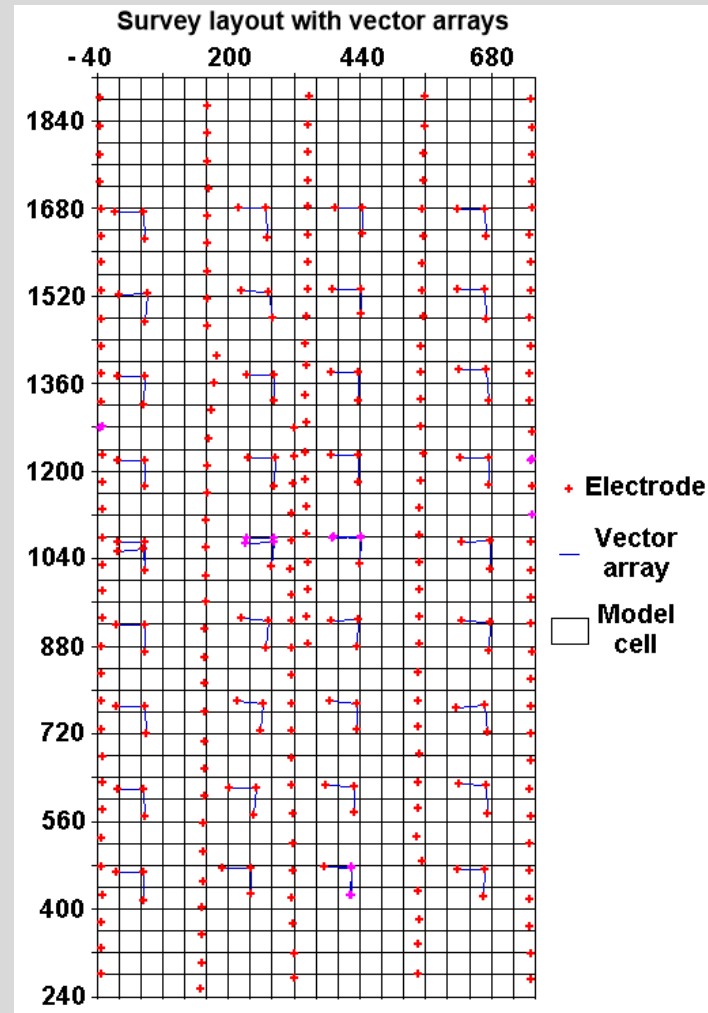
The layout for an I.P. survey by Iris Instruments using interleaved lines of current and potential electrodes is shown below. When treated as conventional pole-dipole arrays, the geometric factors range from about 200 to 70,000,000 m with a number of negative apparent resistivity values.

The inversion had difficulty converging with high data misfits.

The equivalent vector arrays data set had lower geometric factors of 200 to 180,000 m, and the inversion was more stable. The angles (α) between the two potential dipoles range from 82° to 98°.

The FEM complex resistivity method was used for the forward modeling method,

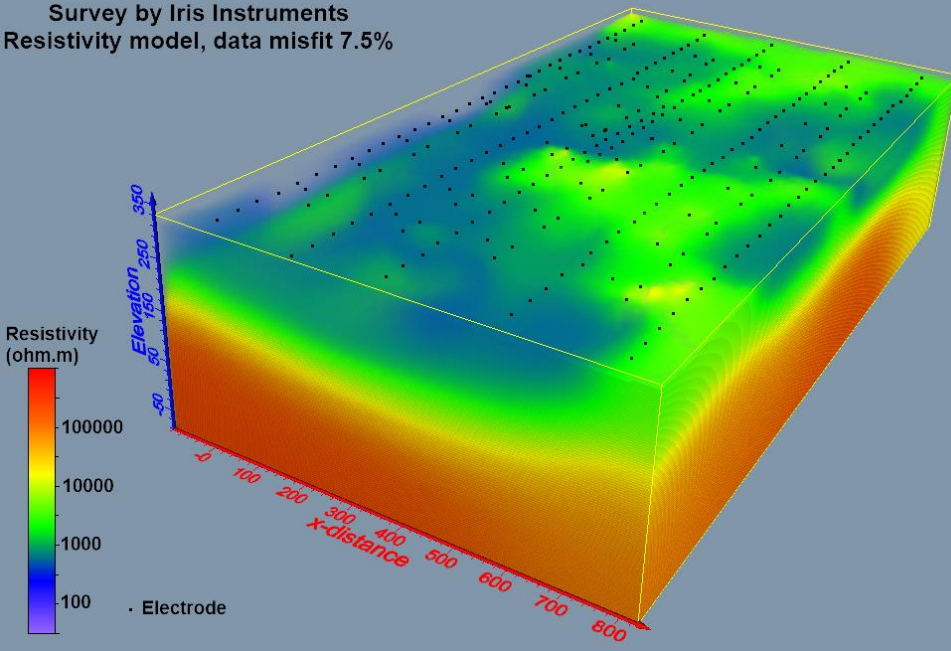
$$\sigma = \sigma_{DC} - i m \sigma_{DC}, \quad \phi = \phi_r + i \phi_i$$



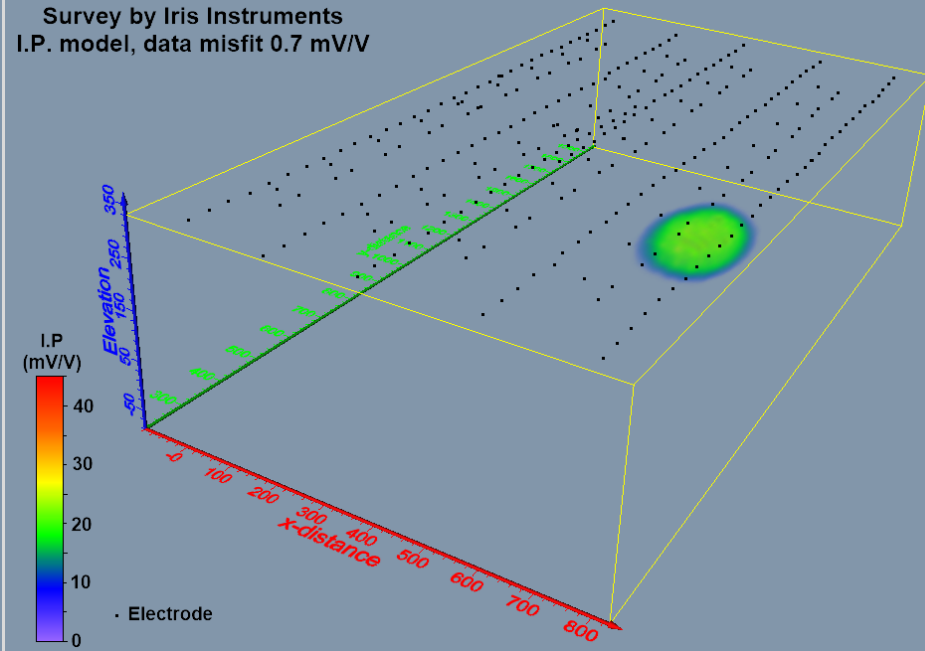
Vector arrays field survey results

The resistivity and I.P. inverse models with misfits of 7.5% and 0.7 mV/V are shown below. The resistivity generally increases with depth, with some local variations in the upper 200 m. A single compact I.P. anomaly with values of over 40 mV/V and diameter of about 150 m is detected at about 50 to 130 m below the surface in the right side of the survey area.

Survey by Iris Instruments
Resistivity model, data misfit 7.5%



Survey by Iris Instruments
I.P. model, data misfit 0.7 mV/V



Structured and unstructured grids

Structured model grid – Use approximately rectangular model grid.

Advantages :- Easier to apply directional roughness filters, 1-D wavelet transform to compress 3-D Jacobian matrix.

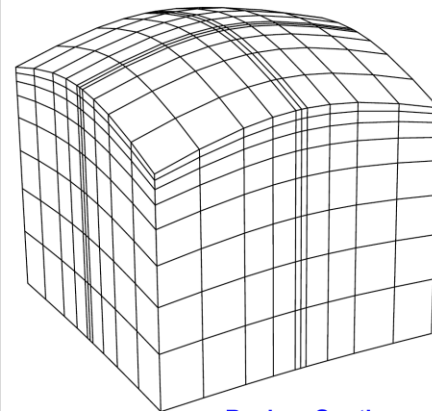
Disadvantages :- Huge 3-D FEM mesh with millions of nodes.
Limitations with huge data sets and models.

Unstructured tetrahedral grid – Use automatic 3-D mesh generator.

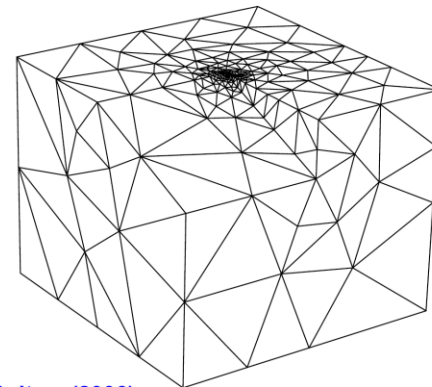
Advantages :- Reduction in number of nodes. Automatic.

Disadvantages :- Difficult to apply directional filters, 1-D wavelet transform. Mesh elements inherently non-symmetrical.

Structured grid



Unstructured grid



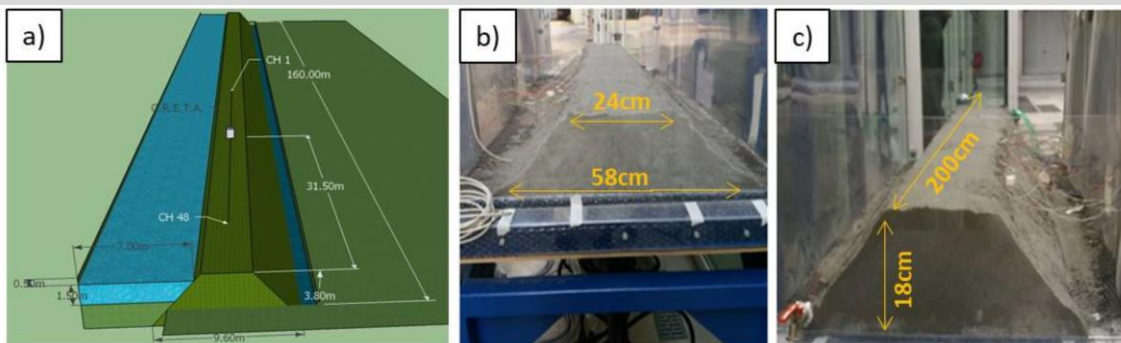
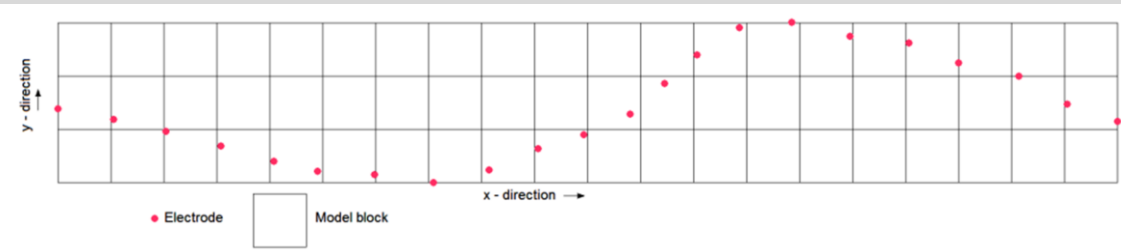
Model grids and finite-element meshes

The subsurface is subdivided into a number of model blocks which are internally homogeneous. The finite-element mesh is much finer than the model grid. Advantages of a structured model grid.

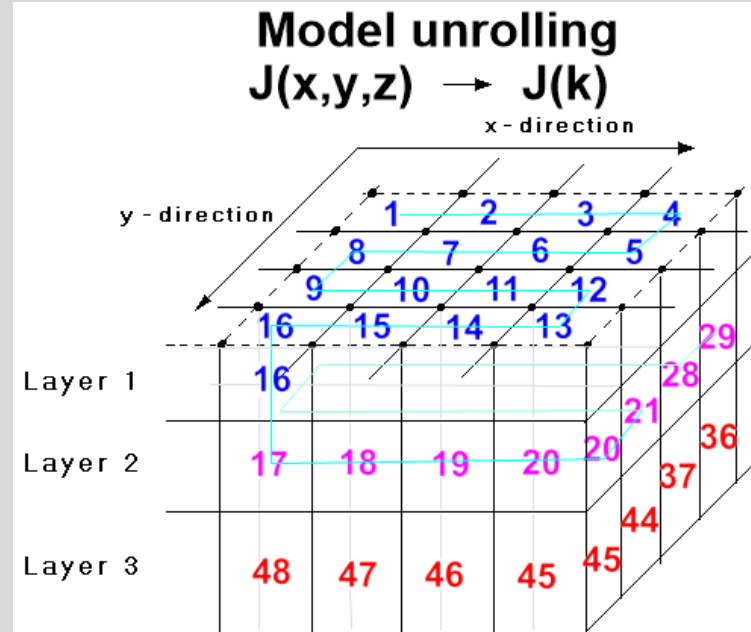
Convert a 3-D Jacobian into a 1-D function.

Model a crooked 2-D line. Use Large y-direction roughness damping factor.

Include off-axis topography, survey along a levee or dam crest.

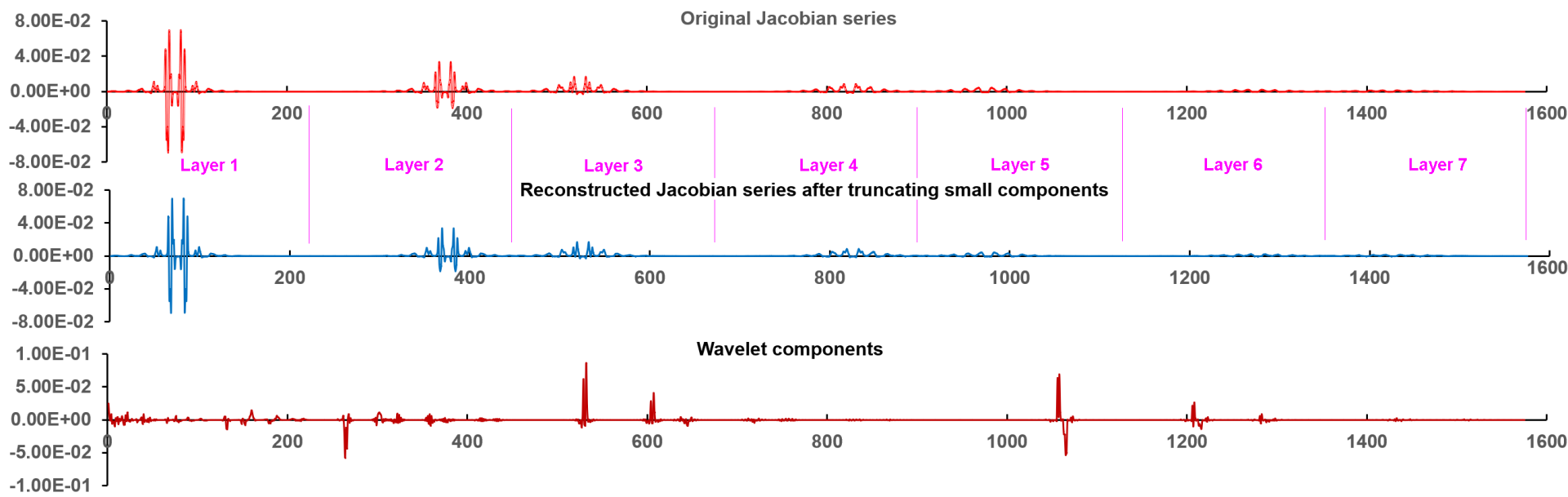


Levee modeling - University of Modena and Reggio Emilia



Wavelet compression with a structured grid

The top plot shows the Jacobian values for a single pole-dipole array ($a=2$, $n=1$) for a model with $15 \times 15 \times 7$ model blocks. Each layer has 225 model blocks. The second plot shows the reconstructed Jacobian values after wavelet components with amplitudes of less than 0.5% of the maximum value were truncated. There are no significant differences between the original and reconstructed Jacobian series. Bottom plot shows the wavelet components. Only a small number of components have significant amplitudes.



Methods for very large data sets and models?

Possible solutions :-

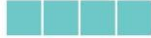
- a) Semi-structured model grid – Use rectangular model grid, but combination of hexahedral, pentahedral/tetrahedral FEM elements.
- b) Use general purpose tetrahedral mesh generator with constraints so they fit within the rectangular model boundaries.
- c) Go highly parallel to accelerate calculations :- GPU, AVX512
- d) Splice and recombine large data sets (divide & conquer).

Still an area of research.

87 FPU :- 8 32-bit registers
1 calculation per clock cycle



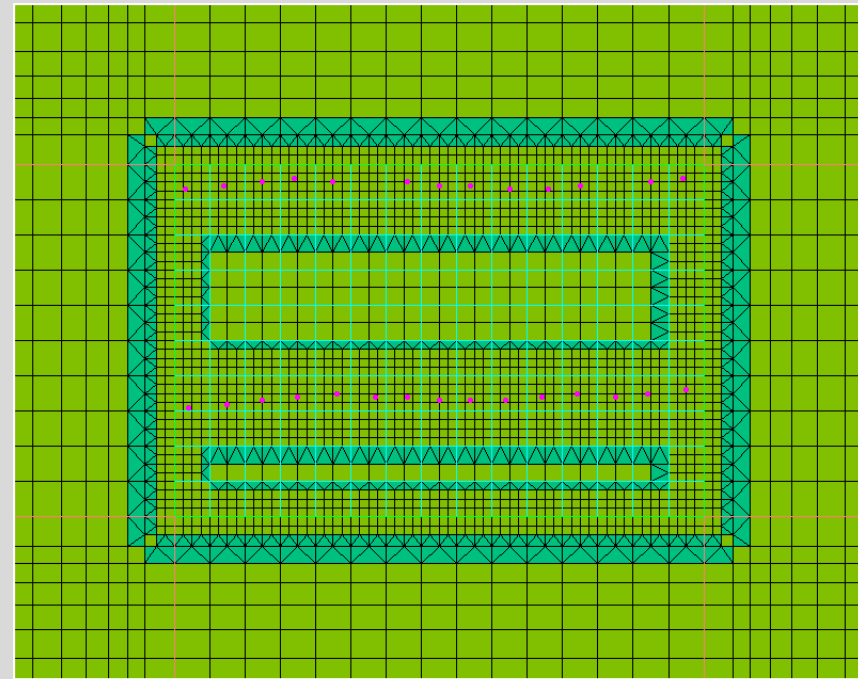
SSE :- 8 4x32 bit registers
4 calculations per clock cycle



AVX2 :- 16 8x32 bit registers
8 calculations per clock cycle



AVX512 :- 32 16x32 bit registers
16 calculations per clock cycle



Model Grid Hexahedral Mesh Pentahedral Mesh

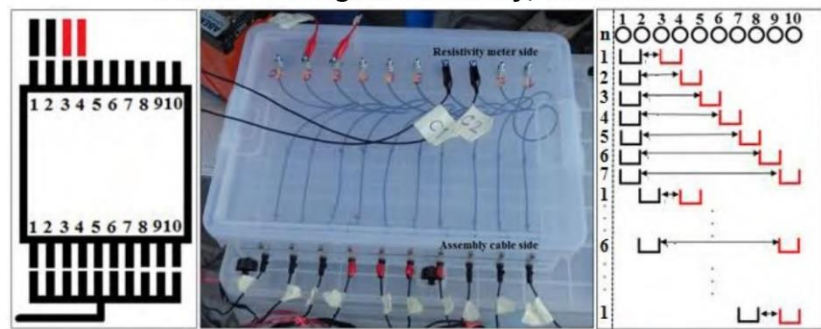
Affordable tech for emerging countries

Multi-electrode systems are still too expensive for many emerging countries. Simple 4-electrode meters are affordable and robust.

Hardware :- Spreadsheet, manual switching box, old seismic cables?

Software :- Free academic programs - BERT, RESINVM3D, others. Generous free 'demo' versions RES2DINVx64 (84 electrodes), RES3DINVx64 (200 electrodes). PC \approx USD1000 (4 core, 16GB RAM).

Prince of Songkla University, Thailand

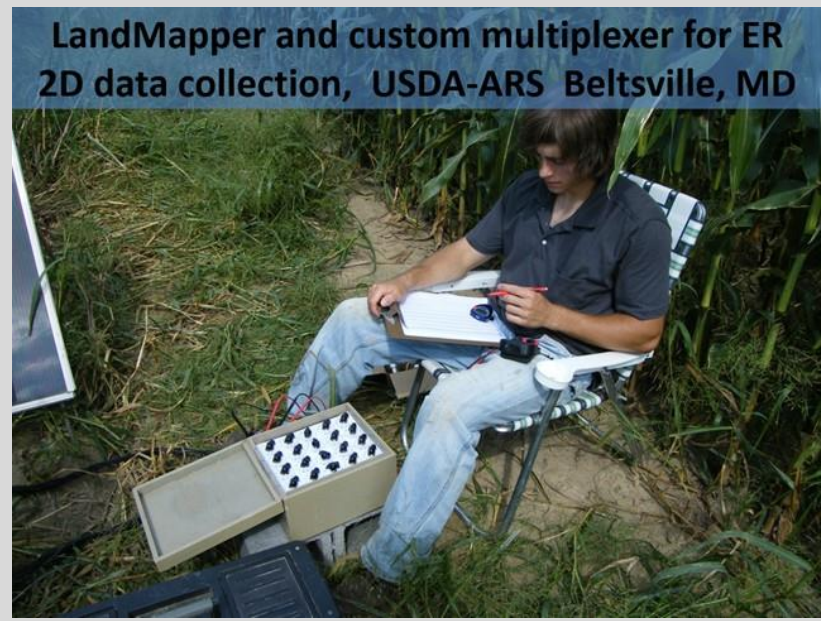


Complete system < USD10,000?

MiniRes ~ USD6000



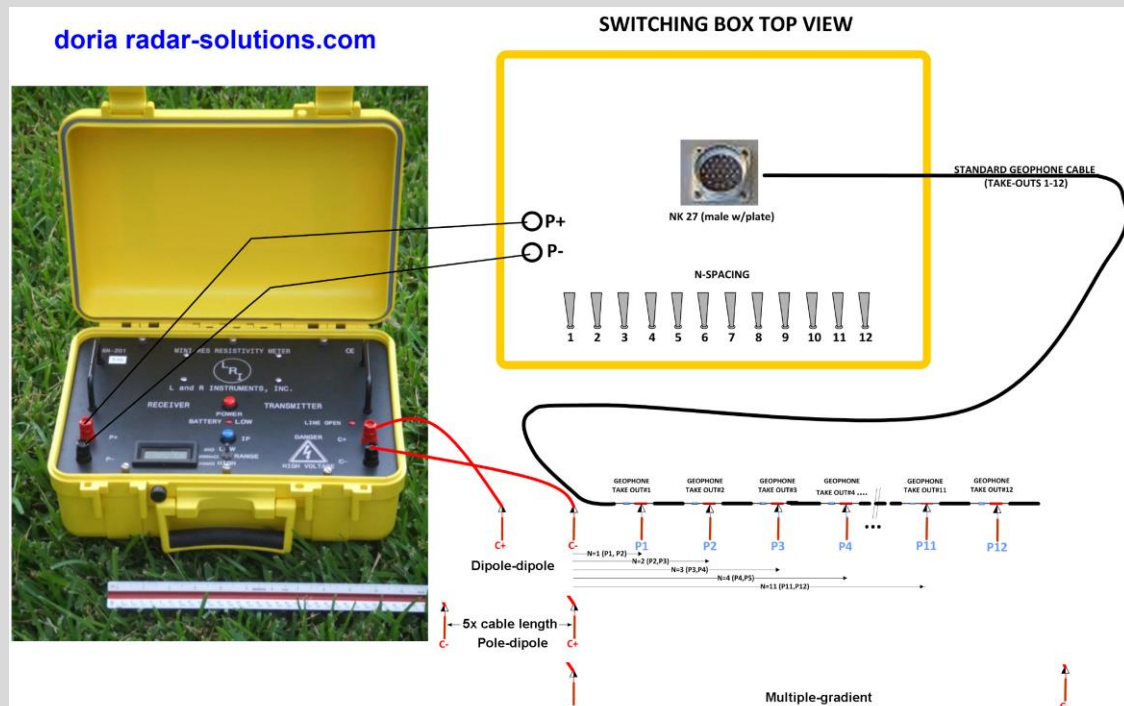
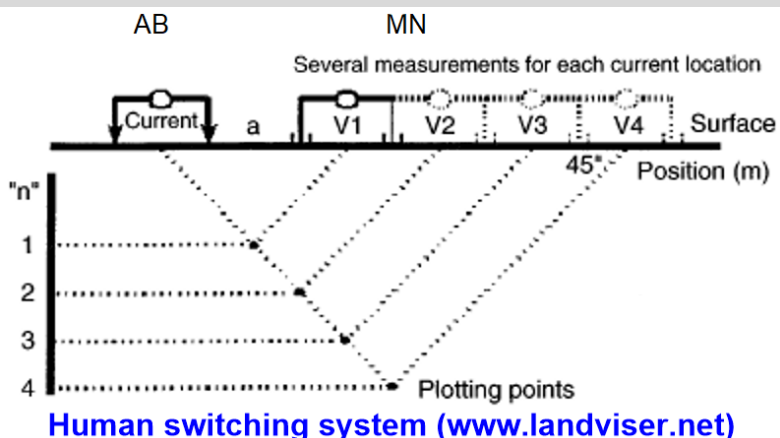
USD2000~3000



Affordable hardware alternatives

1). Standard 4-electrodes meter with spreadsheet and human switching system. Pros :- Simple, no extra hardware needed. Cons :- slow, possible field errors.

2). Mechanical switching box. Pros :- Faster and more flexible. Cons :- Construction needed. Needs robust cable system - use old seismic cables? Simplified switching system with minimal switches and wires - dipole-dipole, pole-dipole, multiple-gradient.



Summary

1. Array optimization methods using the model resolution as the objective function provides an automatic method to find the 'best' arrays for almost any situation. However it needs to be more widely tested in field surveys to refine it.
2. The 4-D time-lapse inversion method can be modified to include additional constraints based on geological data. An emerging field is landslide monitoring where movements of the electrodes must be included.
3. An alternative to processing data from vector arrays is to use the combined measurements instead of individual separate data.
4. For wider impact in emerging countries with water shortage, methods to reduce the costs for ERT surveys are needed. Simpler and cheaper technological solutions could be the answer.

On shoulders of giants

Don Griffiths, Ian Acworth, Ron Barker, The University of Birmingham, UK :- pioneers in ERT

Paul Wilkinson, Jonathan Chambers and others at British Geological Survey, UK :- array optimization and time-lapse

Un. British Columbia, Canada :- theory

Korea Inst. Geosc. And Min. Res., South Korea :- theory

Dale Rucker and Nigel Crooks, HGI, USA :- interesting and challenging data sets

Institute of Mediterranean Studies, Greece :- marine archaeological surveys

Lund University, Sweden :- engineering and environmental surveys

Universidad Nacional Autónoma de México :- Perimeter surveys